2020년 2월
석사학위논문

니켈 foam을 이용한 우수한 고정화 재료 합성 및 고정화효소 특성 분석

조 선 대 학 교 대 학 원

화 학 공 학 과

사 방 지

니켈 foam을 이용한 우수한 고정화 재료 합성 및 고정화효소 특성 분석

Synthesis of Novel Immobilized Materials Based on Nickel Foam and Study on Properties of Immobilized Enzymes

2020년 2월 25일

조선대학교 대학원

화학공학과

사 방 지

니켈 foam을 이용한 우수한 고정화 재료 합성 및 고정화효소 특성 분석

지 도 교 수　　이 중 헌

이 논문을 공학 석사학위신청 논문으로 제출함

2 0 1 9 년　1 0 월

조 선 대 학 교　대 학 원

화 학 공 학 과

사　　방　　지

사방지의 석사학위논문을 인준함

위원장 조선대학교 교 수 신현재 (인)

위 원 조선대학교 교 수 이중헌 (인)

위 원 조선대학교 교 수 이재욱 (인)

2 0 1 9 년 1 1 월

조 선 대 학 교 대 학 원

Contents

List of Tables ····· **IV**

List of Figures ····· **V**

ABSTRACT ····· **VIII**

Ⅰ. Introduction ····· 1

A. Immobilization technology ····· 1

B. Immobilization carrier materials ····· 5

1. Traditional immobilization carriers ····· 5

2. New immobilization carriers ····· 5

C. Carrier materials-PANI, PAMP, TA@$FeCl_3$_$6H_2O$, PDA ····· 7

D. Research outline ····· 13

Ⅱ. Materials and Methods ····· 14

A. Materials ····· 14

1. PANI and PAMP ····· 14

2. TA@$FeCl_3$_$6H_2O$ ····· 14

3. PDA ····· 14

4. Enzyme immobilization and activity assay ····· 14

B. Methods ····· 15

1. Preparation for PANI, PAMP ····· 15

2. Preparation for TA@$FeCl_3$_$6H_2O$ ····· 15

3. Preparation for PDA ····· 15

4. Immobilization of enzymes on different carriers ····· 16

5. Characterizations ····· 19

6. Enzyme loading test ····· 19

7. Enzyme activity assay ····· 21

8. Storage stability of immobilized enzyme ····· 26

9. Application of Micro-PFR with immobilized enzymes ····· 26

a) Micro-PFR process using immobilized GOx ····· 28

(1) Production of gluconic acid using Micro-PFR process ····· 28

(2) Effect of pH, temperature and substrate concentration on Micro-PFR process ····· 32

(3) Response surface analysis of Micro-PFR ····· 35

(4) Study on the operational stability of immobilized enzymes with Micro-PFR ····· 39

b) Micro-PFR process using immobilized LIP ····· 40

Ⅲ. Results and Discussion ····· 42

A. Morphology and size of immobilized GOx/LIP ····· 42

B. Surface chemistry analysis ····· 45

C. Enzyme loading analysis ····· 50

D. Storage stability analysis ····· 52

E. Stability analysis of Micro-PFR ····· 54

1. Operational stability of immobilized GOx ····· 54

2. Operational stability of immobilized LIP ····· 56

Ⅳ. Conclusion ····· 58

References ····· 60

초록 ····· 67

List of Tables

Table 1. Enzyme activity assay ····· 25

Table 2. ANOVA for Response Surface Quadratic model of PDA-GOx ····· 37

Table 3. ANOVA for Response Surface Quadratic model of PAMP-GOx ····· 38

Table 4. The immobilization yield of enzyme onto different carriers (≤±5%) ····· 51

List of Figures

Figure 1. Conventional immobilization technology (a) adsorption, (b) covalent bonding, (c) encapsulation, (d) crosslinking. ····· 2

Figure 2. Chemical structure of polyaniline. ····· 8

Figure 3. The molecular structure of TA@$FeCl_3$_$6H_2O$. ····· 10

Figure 4. The molecular structure of polydopamine. ····· 12

Figure 5. Overview of carrier synthesis and immobilization processes. (a) PANI, (B) PAMP, (c) TA@$FeCl_3$_$6H_2O$, (d) PDA, (e) enzyme immobilization. ····· 17

Figure 6. The effect of immobilized enzyme with different concentration on the reaction efficiency. (a) GOx, (b) LIP. ····· 18

Figure 7. Standard curve for the determination of protein concentration. ····· 20

Figure 8. Glucose oxidase is used for the oxidation of glucose and peroxidase is used for the oxidation of o-dianisidine to a stable and colored product for detection. ····· 22

Figure 9. Enzymatic hydrolysis reaction of 4-nitrophenyl butyrate. ····· 24

Figure 10. PFR reaction system to detect the stability of immobilized enzyme reactor. ····· 27

Figure 11. Standard curve for the determination of hydrogen peroxide (H_2O_2) concentration. ····· 29

Figure 12. The reaction conversion at the different flow rates. (a) PANI, (b) PAMP, (c) TA@$FeCl_3$_$6H_2O$, (d) PDA. ····· 30

Figure 13. The stability of immobilized GOx at the flow rate of 1 mL/min. (a)

PANI, (b) PAMP, (c) TA@$FeCl_3$_$6H_2O$, (d) PDA. ····· 31

Figure 14. Effect of feed glucose concentration on yield. (at 25℃, 1 mL/min) ····· 33

Figure 15. Effect of a. temperature, and b. pH on gluconic acid yield. (● PDA-GOx, ○PAMP-GOx) ····· 34

Figure 16. Response surface graph of gluconic acid yield (%) with temperature and pH. (PDA-GOx) ····· 37

Figure 17. Response surface graph of gluconic acid yield (%) with temperature and pH. (PAMP-GOx) ····· 38

Figure 18. Standard curve for the determination of 4-nitrophenol concentration. (pH 6.5) ····· 41

Figure 19. 4-Nitrophenolate conversion using Micro-PFR. ····· 41

Figure 20. SEM images of (a) Ni-foam, (b) Ni-foam-GOx, (c) Ni-foam-LIP, (d) Ni-foam-PANI, (e) PANI-GOx, (f) PANI-LIP, (g) Ni-foam-PAMP, (h) PAMP-GOx, (i) PAMP-LIP, (j) Ni-foam-TA@$FeCl_3$_$6H_2O$, (k) TA@$FeCl_3$_$6H_2O$-GOx, (l) TA@$FeCl_3$_$6H_2O$-LIP, (m) Ni-foam-PDA, (n) PDA-GOx, (o) PDA-LIP. ····· 44

Figure 21. FTIR-ATR spectra of PANI/Ni-foam, PAMP/Ni-foam and Fe_3O_4. ····· 47

Figure 22. FTIR-ATR spectra of tannic acid, $FeCl_3$_$6H_2O$ and TA@$FeCl_3$_$6H_2O$/Ni-foam. ····· 48

Figure 23. FTIR-ATR spectra of dopamine and PDA/Ni-foam. ····· 49

Figure 24. Storage stabilities of immobilized (a) GOx, (b) LIP 2 mg/mL at 4℃. (● Ni-foam, ○ PANI, ▼ PAMP, △ TA@$FeCl_3$_$6H_2O$, ■ PDA) ····· 53

Figure 25. The operational stability of the immobilized GOx in a Micro-PFR under optimal conditions. ····· 55

Figure 26. The operational stability of the immobilized LIP in a Micro-PFR at pH 6.5 and room temperature. ····· 57

ABSTRACT

Synthesis of Novel Immobilized Materials Based on Nickel Foam and Study on Properties of Immobilized Enzymes

XIE FANGZHI

Advisor: Prof. Lee, Jung–Heon, Ph.D.

Department of Chemical Engineering

Graduate School of Chosun University

With the continuous development of biotechnology, materials, chemistry and other modification methods, new materials continue to emerge, enriching the carrier sources of immobilization technology researches. Nickel foam (Ni-foam) was used as the carrier material, because of its being inexpensive, easy to handle and sponge-like porous structure makes it well suited as a base carrier material. In this study, the surface of Ni-foam was coated with various polymer materials, including polyaniline nanofibers (PANI), polyaniline magnetic particles (PAMP), and tannin iron ion complex ($TA@FeCl_3\_6H_2O$), polydopamine (PDA). They have functional groups, thereby making it easier to immobilize the enzyme with the chemical cross-linking method. PANI, PAMP, $TA@FeCl_3\_6H_2O$, and PDA were synthesized in one step and subsequently coated on Ni-foam. Previously, these polymer materials were used in the form of dispersed particles as enzyme immobilizers. However, after Ni-foam was coated with these materials, it was easier to separate them from the reaction solution and control the reaction. The immobilized enzymes and its carrier properties were characterized by using fourier transform infrared (FTIR-ATR) spectrophotometer, scanning electron micro-

scope (SEM), and UV/Visible spectrophotometer.

The FTIR-ATR spectroscopy results showed that the polymer particles synthesized by one-step method were our desired polymer materials and provided a direct proof for the synthetic process of these polymer materials. The SEM images showed the various nanofibrous forms which had increased surface area for enzyme immobilization.

The stabilities of immobilized lipase (LIP) and glucose oxidase (GOx) were analyzed . The results showed that, the activity of GOx immobilized Ni-foam almost disappeared after a month. However, the residual activities of PANI, PAMP, TA@$FeCl_3$_$6H_2O$, and PDA were 50.9%, 70.4%, 72.1%, 73.4%, respectively. The initial activity of immobilized LIP on bare Ni-foam was higher than that of PAMP, PANI, PDA coatings, but the stability was not good. Immobilized LIPs on TA@$FeCl_3$_$6H_2O$ was the most stable and had the best residual enzyme activity, followed by PDA, PAMP. After one month, the residual activities of immobilized enzymes on bare Ni-foam, PANI, PAMP, TA@$FeCl_3$_$6H_2O$, and PDA were 83.1%, 73.3%, 93.4%, 90.1%, and 98.3%, respectively.

A PFR micro reactor with a capacity of 600 μL was developed, and the nickel foam with immobilized enzyme was used in a tubular reactor. The experimental results showed that PDA-GOx and PAMP-GOx have good operational stabilities. The glucose conversion with PDA-GOx decreased from 84.6±4.7% to 18.4±2.3% after 172 hours, while that of PAMP-GOx from 82.1±1% to 22.2±4.4%. For LIP, the hydrolysate of substrate 4-NPB was greatly affected by pH, so the pH was fixed to 6.5, and micro PFR was used to detect its operation stability at room temperature. The results showed that the conversion did not change after 24 days continuous operation of.

In summary, the modification of Ni-foam did not only increase the stability of the enzyme reaction process, but also make the process economical feasible.

Keywords: Polyaniline nanofibers (PANI), polyaniline magnetic particles (PAMP), tannin iron ion complex (TA@$FeCl_3$_$6H_2O$), polydopamine (PDA), nickel foam (Ni-foam), lipase (LIP), glucose oxidase (GOx)

I. Introduction

Enzyme is widely used in various fields because of its easy production, substrate specificity, high selectivity and high activity. Moreover, the enzyme itself can be degraded by microorganisms, in line with the requirements of green chemistry. However, it is well known that enzymes also have the following problems. (1) Once the enzyme is separated from the cell, its activity decreases rapidly, and it is sensitive to external factors, such as temperature and pH, and is also extremely easy to be inactivated due to changes in reaction conditions; (2) due to its complicated process of separation and purification, the enzyme is more expensive than ordinary catalysts, so the large-scale preparation and application become a major problem; (3) most of the enzymes are soluble in water, and the reaction in an aqueous solution causes the contamination of the product and is difficult to separate, recover and re-use [1, 2]. Immobilization of the enzyme is to overcome the above disadvantages, so that the enzyme catalytic reaction can be stabilized in a heterogeneous reaction, like a chemical catalytic reaction, and is easy to recycle and reuse.

Immobilization of an enzyme means that the enzyme is immobilized on a less soluble carrier material by physical or chemical processes, which remains catalytically active and can be recovered and tested repeatedly [3]. Enzyme immobilization is mainly carried out from two parts: immobilization technology and immobilization carrier materials [4].

A. Immobilization technology

The first scientific observation that led to the discovery of immobilized enzymes was made in 1916 [2]. After several decades of development, a variety of immobilized technologies have emerged, which are derived from the traditional immobilization technology. Four basic immobilization technologies, adsorption, covalent bonding, encapsulation, crosslinking [5], are summarized as shown in Figure 1.

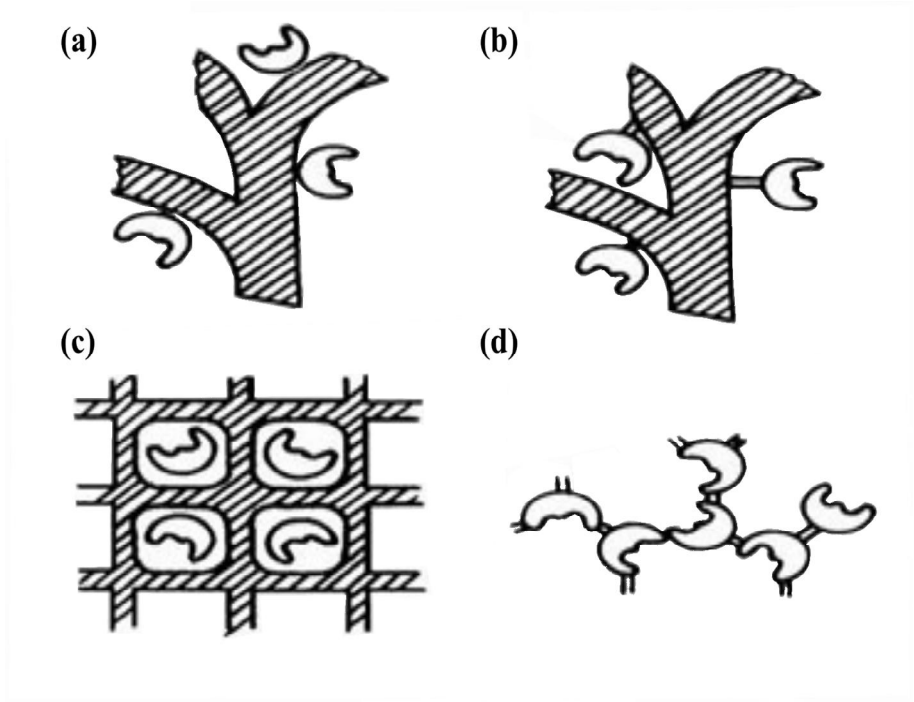

Figure 1. Conventional immobilization technology (a) adsorption (b) covalent bonding (c) encapsulation (d) crosslinking.

Adsorption is the simplest and most advanced method of enzyme immobilization. It uses some weak bonds to immobilize the enzyme on the carrier, such as van der Waals force, hydrophobic interaction and surface tension. The advantages of immobilized enzyme preparation by adsorption method are simple operation, low restriction on carrier and enzyme, high recovery rate and efficiency of enzyme activity, low cost. But at the same time, the immobilized enzyme is unstable and easy to fall off. It should be noted that the carrier may have some adsorption on the product [6].

Covalent bonding is one of the most widely used immobilization methods, which refers to the process of amino acid residues on enzyme covalent bonding with the active groups on the surface of carrier. This method generally requires the carrier to contain more chemical groups or have stronger modification to generate chemical bond coupling with enzyme molecules. Common chemical bonds include isourea bond, diazo bond, epoxy group and alkane, carboxyl group, etc [7]. Covalent binding method is a relatively simple method, which has strong stability and is not easy to lose enzyme molecules and desorb. However, the functional modification of enzyme changes the conformation of enzyme molecule, resulting in the decrease of enzyme activity [8].

Entrapment means that the enzyme is physically embedded in the matrix with porous or network structure, and the enzyme is immobilized by adjusting the pore size of the matrix. This method does not react with the carrier, it does keep the molecular conformation of the enzyme, improve the mechanical stability of the enzyme, along with reduce the leaching of the enzyme, but limits the diffusion of the enzyme. Moreover, the size of matrix and product molecules is also limited, which is too large for to pass through the matrix.

Crosslinking is an irreversible method to form covalent bonds between enzyme molecules using bifunctional or multifunctional crosslinkers [9]. The commonly used crosslinking agents are glutaraldehyde [10, 11], hexamethylene diisocyanate, maleic anhydride, bisazobenzene, isocyanate derivatives, etc. Because of the multi-functional structure of the crosslinking agent, the crosslinking reaction may occur in the active center of the enzyme, reducing or deactivating the activity of the enzyme. In addition, the immobilized enzyme crosslinks formed by simple crosslinking have no carrier and poor

mechanical properties. Therefore, the crosslinking method combined with other immobilization methods can obtain better immobilization effect [7].

At present, many enzyme immobilization methods derived from basic immobilization methods have been reported.

B. Immobilization carrier materials

1. Traditional immobilization carriers

Common traditional carrier materials, such as silica, activated carbon and other inorganic materials, with high specific surface area and porous structure which are more suitable for immobilization. For example, a glucose biosensor with higher performance is made by immobilizing glucose oxidase on silica with smaller particle size [12], and glucose isomerase immobilized on a silica carrier is used to produce isoglucose [13]. In addition, silica is modified into functional silica carrier with high active functional group, which has been widely used in enzyme immobilization. Horseradish peroxidase is immobilized on functionalized NH_4-Fe_3O_4/SiO_2 particles to degrade 2, 4-dichlorophenol [14], and starch glucosidase is immobilized on activated carbon to make it have excellent catalytic activity and reusability [15].

Organic materials such as polystyrene, chitosan, sodium alginate are also traditional materials. In practical application, the invertase from *Saccharomyces cerevisiae* is covalently immobilized on macromolecular polystyrene for the production of a mixture of glucose-fructose [16]. Lipase is immobilized on chitosan by adsorption for the production of n-butyl butyrate [17]. *Saccharomyces cerevisiae* is immobilized on the chitosan for the production of (R)-mandelic acid [18], β-glucosidase is immobilized on the sodium alginate to prepare the aroma of tea beverages [19], etc.

To sum up, the traditional immobilization not only carriers have high specific surface area and porous structure, which is easy to be modified to form functional carriers, but also has good mechanical properties and stability. And enzyme immobilization carriers have good application in actual project.

2. New immobilization carriers

In recent years, in order to enhance the loading capacity, stability and activity of enzyme, with the cost reduced, researchers have conducted varieties of researches on immobilized new carriers such as nano carriers, magnetic carriers, and composite carriers. The high specific surface area of nanoparticles makes those carriers a hot topic. In ad-

dition, studies have shown that nanoparticles can improve the stability and performance of enzyme as carrier materials [20]. Compared with the traditional immobilization carriers, the enzyme nanoparticles make it easier to synthesize under safe conditions, and can obtain uniform core-shell nanoparticles, which has high practicability [21, 22]. For example, the triacylglycerol lipase immobilized on aldehyde-modified nano-SiO_2 exhibits excellent stability [23], and the biosensor prepared by immobilizing glucose oxidase on gold nano-sized particles has good reproducibility and stability [24].

The magnetic carrier material appears due to the problem of immobilized enzyme separation, which makes the enzyme immobilized on the carrier material easy to be separated by the magnetic field provided by the outside. Most of the magnetic carrier materials are made from metal and its oxides, and the most commonly used one is iron oxide. However, some studies have shown that individual magnetic nanoparticles may be unstable and aggregate under certain reaction conditions, thus reducing the reaction efficiency [25]. Therefore, in order to resolve this problem, it can be coated by a synthetic polymer, which is encapsulated to protect the magnetic nanoparticles, i.e. to form a composite carrier material [26]. For instance, the immobilization of α-chymotrypsin on the magnetic nanoparticles modified by polydopamine shows good stability and reusability, and that more than 84% activity after 10 cycles of use [27]. The immobilization of invertase, β-galactosidase and trypsin on the magnetic diatomaceous material coated with polyaniline is used in industrial production, and the obtained composite exhibits good magnetic properties and make it easy to recycle [28].

There are many types of carrier materials for enzyme immobilization, all of which are improving the stability and reusability of enzyme and reducing the cost of industrial production. Moreover, in order to improve and compensate certain defects, various hybrid composite carrier materials, namely novel carrier materials, have been invented.

C. Carrier materials-PANI, PAMP, TA@$FeCl_3$_$6H_2O$, PDA

The carrier material used in this study is nickel foam (Ni-foam), which is inexpensive and easy to experiment with. Its unique pore structure, low pressure input hole, inherent tensile strength and thermal shock resistance make Ni-foam the main object of this study. In addition to being used as enzyme carrier in this paper, it is also active in other fields. Composite porous materials, ranging from sponge to porous metal nickel, can be used as electrode materials to support CoO-Li_2O in the field of electrochemistry, such as NiSe nanowire film, NiO/polyaniline film, etc. It can also be used as filter materials and precious metal replacement recovery.

SEM image showed that the surface of Ni-foam was very smooth, which is not conducive to enzyme immobilization. For this purpose, polyaniline nanofibers (PANI), polyaniline magnetic particles (PAMP), tannic acid@$FeCl_3$_$6H_2O$ (TA@$FeCl_3$_$6H_2O$) and polydopamine (PDA) coatings were used to modify the surface morphology of Ni-foam.

PANI is synthesized by rapid mixing the aniline monomer and ammonium persulfate. Adding excessive ammonium persulfate as initiator to prevent the overgrowth of polyaniline. As for enzyme immobilization, it provides an interesting nanostructure (as shown in Figure 2) [29, 30] can provide a large surface area for the attachment of enzymes, which can lead to high volumetric enzyme activity. More precisely, it is a rod-shaped nano polymer. Polyaniline has the advantages of its easy of synthesis, low cost monomer, tunable properties, good semi-conductivity, high conductivity activity, good environmental stability and so on. It is one of the most widely used conductive polymers [31, 32].

PAMP is synthesized by adding Fe_3O_4 in the process of PANI synthesis. By changing only the content of magnetic material, the magnetic intensity of PAMP can be totally changed [33]. In this study, magnetic Fe_3O_4 particles also play a role of increasing friction. Therefore, the synthesized PAMP is more easily adsorbed on Ni-foam.

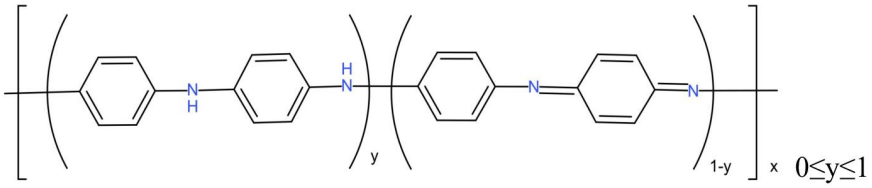

(a)

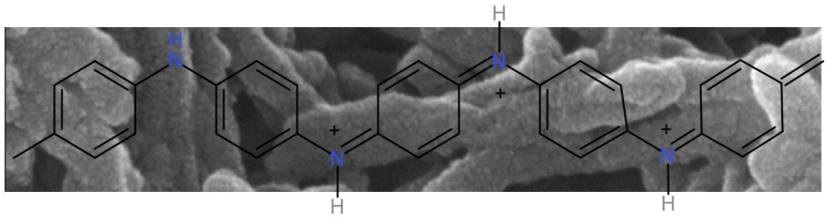

(b)

Figure 2. Chemical structure of polyaniline [32].

TA, a special form of tannin, is a high-molecular-weight polyphenol. It contains a large number of phenolic and dihydroxymethyl ester groups which are covalently linked to the central glucose core. It is also ubiquitous in nature and exhibits anti-oxidation, anti-bacterial, antimicrobial, together with anticarcinogenic properties. Furthermore, TA has unique structural properties which promote the interaction with various materials along with reaction pathways, including electrostatic, hydrogen bond, and hydrophobic interaction. And metal chelation is a salient feature of TA, upon which it acts as a polydentate ligand for metal ion coordination [34]. Usually, metal chelates made by condensing Fe^{3+} ions and natural polyphenol tannins from aqueous solution can coat flat surfaces and change surface morphology. Three galloyl groups from TA can react with each Fe^{3+} ion to form a stable octahedral complex, allowing each TA molecule to react with several Fe^{3+} centers to form a across-linked film. In a certain range, the higher content of iron ion has, the thicker the film is formed. For TA, TA@$FeCl_3$_$6H_2O$ composite coated on the Ni-foam is easy to fall off because of the over thickness, but only enough thickness can be conducive to immobilized enzyme [35].

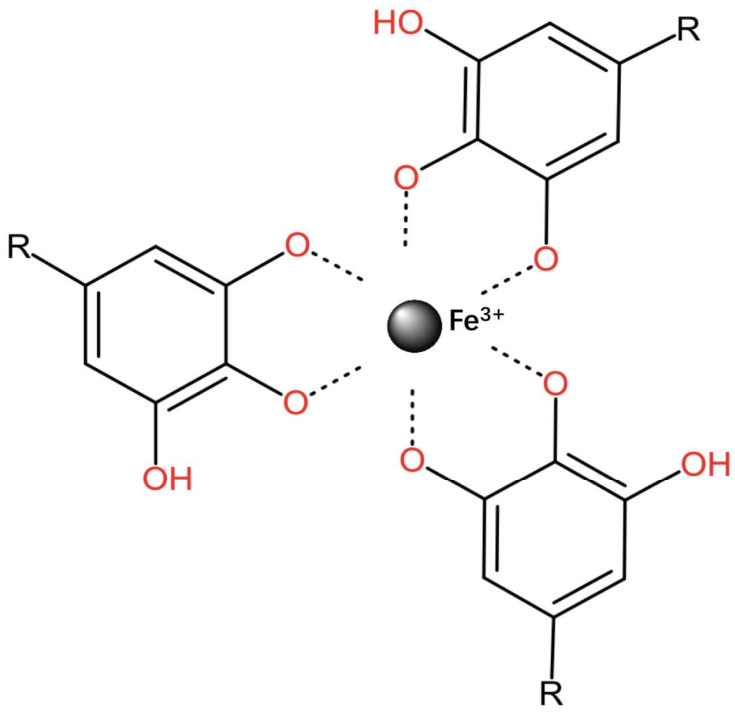

Figure 3. The molecular structure of TA@$FeCl_3$_$6H_2O$ [36].

Dopamine, a molecule with both catechol and amino groups, can self-polymerize to form a conformal coating on various surfaces in an oxidizing agent and weak alkaline environment. Polydopamine (PDA) has many properties, such as versatile adhesive properties for inorganic and organic substrates and nanostructure, hydrophilic, non-toxic properties, self-reducing ability, and in situ N-doping through carbonization for enhancing catalytic performance [37, 38]. Therefore, polydopamine which contains a large number of reactive functional groups can adhere to a variety of substrate materials to form PDA coatings. In this paper, the one-step controllable method was used to prepare the polydopamine particles in ethanol solution. The particle size was controlled by controlling the concentration of NH_4OH, and the required particles were obtained.

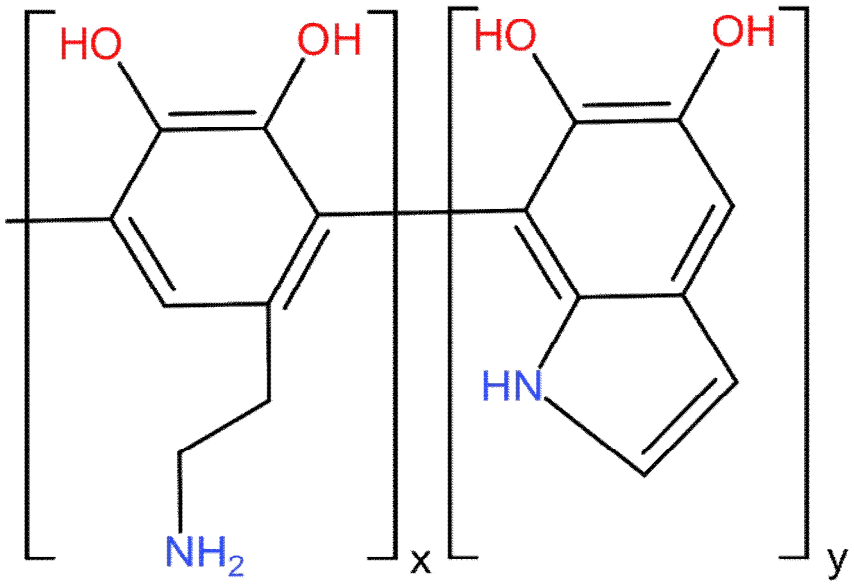

Figure 4. The molecular structure of polydopamine.

D. Research outline

The desired polymer is prepared with a simple and controllable synthesis method, and nickel foam is added during the synthesis process, adjusting the shaker rotation speed to 200 rpm. On one hand, the reaction solution was better mixed. On the other hand, the synthesized particles were physically adsorbed to nickel foam to finish coating. The surface morphology of the composite was examined by scanning electron microscopy (SEM). Images were also obtained before and after coating, enzyme immobilization. And using fourier infrared spectroscopy to identify whether the synthesized polymer was required for this study, which could provide strong and direct evidence for the synthesis process. The enzyme adsorption, precipitation, and crosslinking (EAPC) method was used because it could increase the amount of enzyme immobilization by adding ammonium sulfate to precipitate enzyme before crosslinking. What is more, the enzymes used in this study were glucose oxidase and lipase, its activity and store stability were studied with a simple and controllable color development method. A micro plug flow reactor was fabricated by using a circular tube, and its operational stability was measured in the same manner as above.

II. Materials and Methods

A. Materials

1. PANI and PAMP

Hydrochloric acid was purchased from Duksan Pure Chemicals CO. Ltd. Aniline, iron (Ⅱ, Ⅲ) oxide and ammonium persulfate was purchased from Sigma Chemical Co. (St. Louis, MO, USA).

2. TA@$FeCl_3$_$6H_2O$

Tannic acid was purchased from Sigma Chemical Co. (St. Louis, MO, USA). Iron (Ⅲ) chloride hexahydrate was purchased from Junsei Chemical Co., Ltd.

3. PDA

Dopamine hydrochloride was purchased from Sigma Chemical Co. (St. Louis, MO, USA). 94% ethanol and ammonium hydroxide (NH_4OH) was purchased from DC Chemical CO., Ltd.

4. Enzyme immobilization and activity assay

Glucose oxidase (GOx) from *Aspergillus niger* was purchased from Biochemica, o-dianisidine dihydrochloride, glutaraldehyde and horseradish peroxidase were purchased from Sigma Chemical Co. (St. Louis, MO, USA). D(+)-glucose was purchased from Junsei Chemical Co., Ltd. Ammonium sulfate was purchased from Duksan Pure Chemicals CO., Ltd. Lipase from *Candida rugose* and 4-nitrophenyl butyrate approx. 98% was purchased from Sigma Chemical Co. (St. Louis, MO, USA). N, N-Dimethylformamide was purchased from Junsei Chemical Co., Ltd. Bradford reagent for 0.1~1.4 mg/mL protein was purchased from Sigma-Aldrich. Hydrogen peroxide (30~32%) was purchased from Oriental Chemical Industries.

B. Methods

1. Preparation for PANI, PAMP

Polyaniline was synthesized by mixing 7.5% of aniline and 0.1 M of ammonium persulfate (APS) in 1 M hydrochloric acid and shaking it vigorously. It is worth noting that in order to make the coating better, Ni-foam was added during the reaction process, that is, 0.1 g of Ni-foam was added to the 7.5% aniline solution when the reaction started. And when its color changed to dark green, it was put on the shaker, where it was shaken at 200 rpm at room temperature for overnight. The Ni-foam was washed with distilled water to eliminate the remaining HCl and free nanoparticles until the color of distilled water remained unchanged [29]. For PAMP, in the process of polyaniline synthesis, 1 g of Fe_3O_4 (Ⅱ, Ⅲ) was added to APS solution to achieve the purpose of synthesizing magnetic nanoparticles.

2. Preparation for TA@$FeCl_3$_$6H_2O$

The Ni-foam was coated with TA@$FeCl_3$_$6H_2O$ coordination complexes as following: the Ni-foam was placed in tannic acid aqueous solution of 0.04 g/mL and then placed on the shaker at room temperature for 30 minutes at 200 rpm. 0.012 g/mL $FeCl_3$_$6H_2O$ aqueous solution (pH about 4) was added to the tannic acid solution containing Ni-foam with a volume ratio of 1:1 [35], and shaken at room temperature for 16 hours at 200 rpm [39]. It can be clearly observed that the color of the solution after reaction was purple black. Therefore, the Ni-foam collected was washed with distilled water until the color of the distilled water did not change, and then stored in distilled water for use.

3. Preparation for PDA

The synthesis of PDA spheres was carried out in a water-alcohol mixed solvent. The Ni-foam was coated with PDA as following: 40 mL 30% ethanol solution was prepared, added Ni-foam and 0.2 mL NH_4OH (28~30%), shaken at 200 rpm for 30 minutes at room temperature. And then, 0.5 g of dopamine hydrochloride was added to the mixed solution, and the color immediately became light gray [40]. After 24 hours,

the color changed to dark gray. The Ni-foam was then recovered and washed with distilled water until the color of the distilled water did not change.

4. Immobilization of enzymes on different carriers

Based on other research results [41, 42], the EAPC method is more effective than other immobilization methods because of precipitation. Therefore, the immobilization effect is more significant and this immobilization method is applied in the study. The specific steps are as follows: the carrier Ni-foam was firstly washed with 100 mM sodium phosphate buffer (pH 7.0) for 3 times, and then decant solution. 0.2 mg/mL (and 2 mg/mL) GOx solution (dissolved in 100 mM PB buffer) and ammonium sulfate (final concentration is 35%) were added, and then it was precipitated in a shaker at 200 rpm for 30 minutes at room temperature. Then, glutaraldehyde was added (the final concentration was 0.5%) [42] for crosslinking the precipitated GOx at 4℃ for 17 hours at 50 rpm. Finally, decant solution and the enzyme-immobilized carrier was washed by 100 mM, pH 7.0 PB buffer for 5 minutes at 200 rpm. And decant solution was then washed with 100 mM Tris-HCl (pH 7.9) for 5 minutes at 200 rpm, and incubated with 100 mM Tris-HCl (pH 7.9) for 30 minutes at 200 rpm to un-react aldehyde groups [29]. Finally, the sample was washed with 100 mM, pH 7.0 PB buffer as the first washing step for 5~10 times and stored in PB buffer at 4℃. The immobilization method of LIP is the same as above.

According to the preliminary measurement (as shown in Figure 6), the enzyme activity immobilized by the enzyme solution with a concentration of 2 mg/mL was significantly higher within the allowable economic benefits, so the immobilized enzyme of this specification was uniformly used in the subsequent experiments.

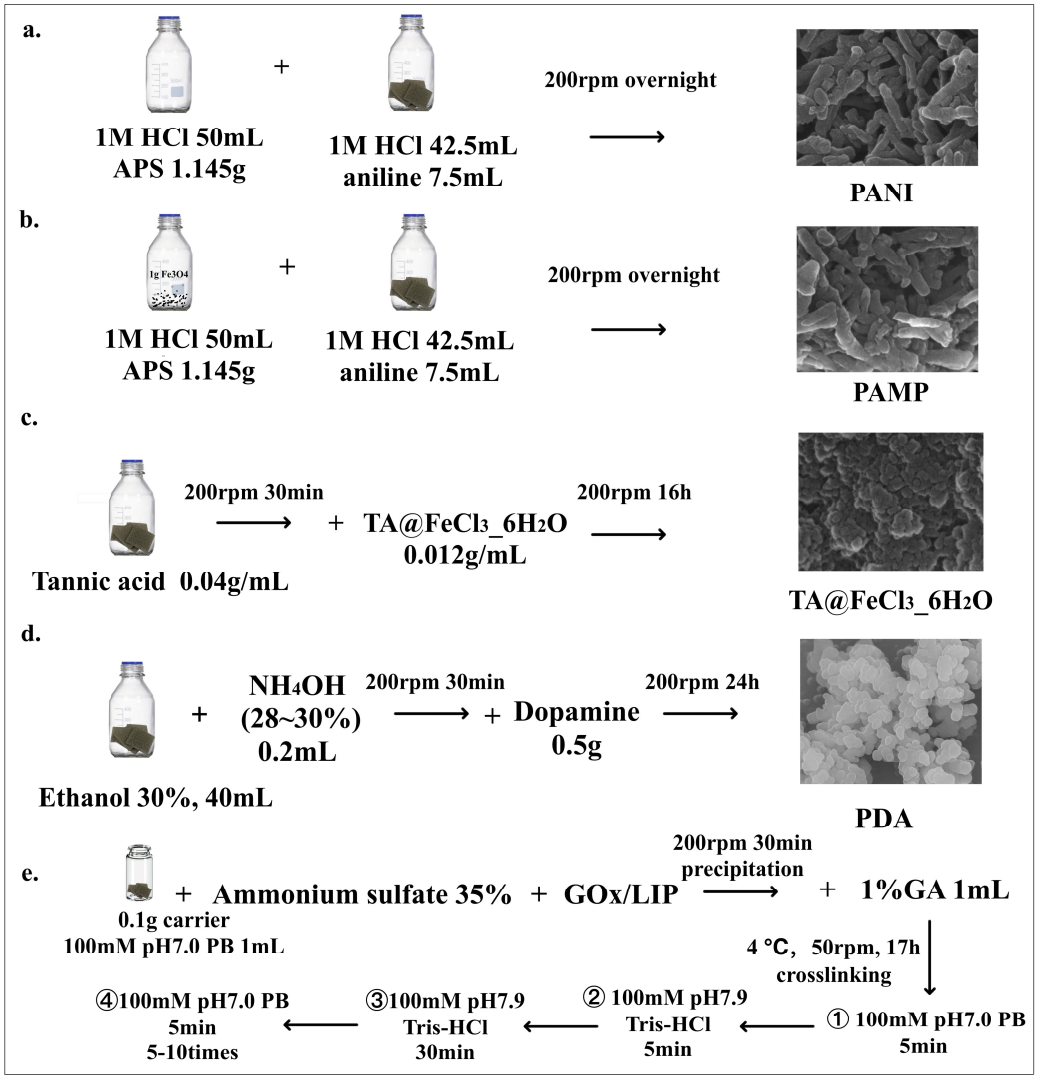

Figure 5. Overview of carrier synthesis and immobilization processes. (a) PANI, (b) PAMP, (c) TA@$FeCl_3$_$6H_2O$, (d) PDA, (e) enzyme immobilization.

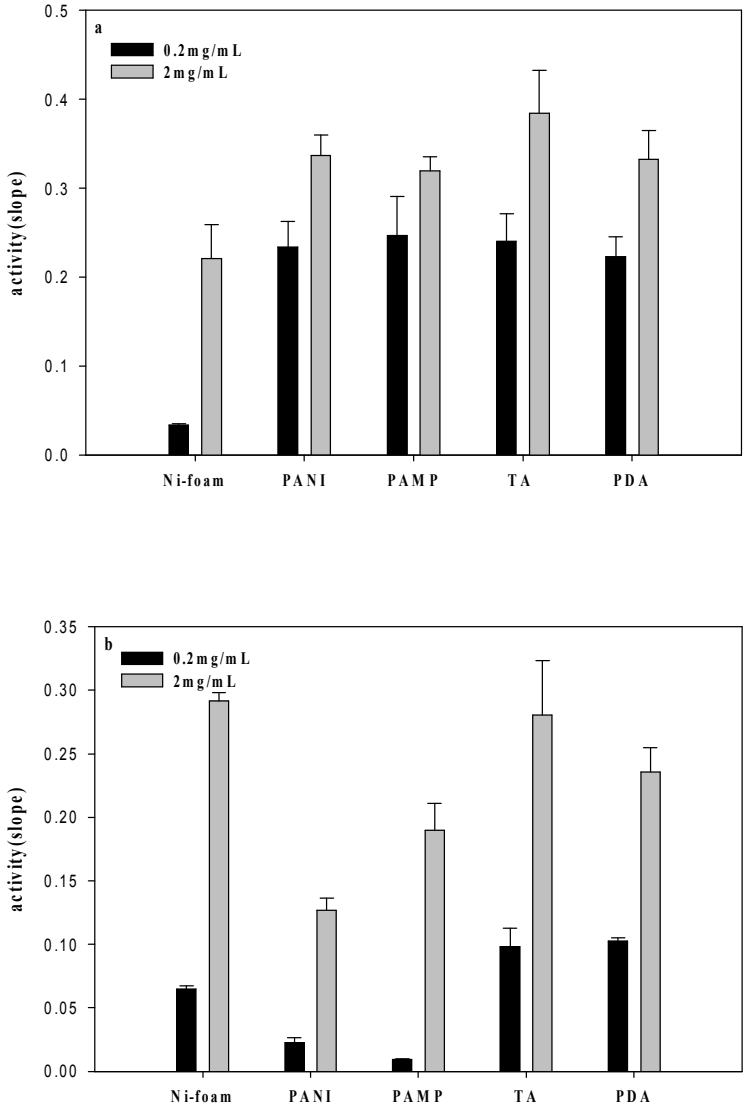

Figure 6. The effect of immobilized enzyme with different concentration on the reaction efficiency. (a) GOx, (b) LIP.

5. Characterizations

Scanning electron micrographs (SEM) of the prepared carriers before and after enzyme immobilization were carried out on a Gemini 500 + EDS (Oxford) scanning electron microscope under the conditions of voltage 15.00 kV and 100.00k×, and coating 60 seconds under 20 mA conditions before scanning electron microscopy. Fourier transform infrared (FTIR) spectra of the carriers were conducted with a FTIR spectrophotometer (Affinity-1, Shimadzu) and ATR.

6. Enzyme loading test

The enzyme loading was carried out with the protein quantitative method to determine the content of each immobilized enzyme in the study. Protein concentration was measured by using the bradford, UV/Visible spectrophotometer (Ultrospec 2100 pro). In order to determine the amount of immobilized enzyme on the existing carrier, the amount of protein in buffer before and after immobilization was measured and calculated. 1.5 mL of bradford reagent was added to the cuvette, mixed with 0.05 mL of the sample, incubated at room temperature for 5 minutes, and finally with the absorbance determined at 595 nm. Standard calibration curve for BSA in the range of 0.1~1.4 mg/mL as shown in Figure 7.

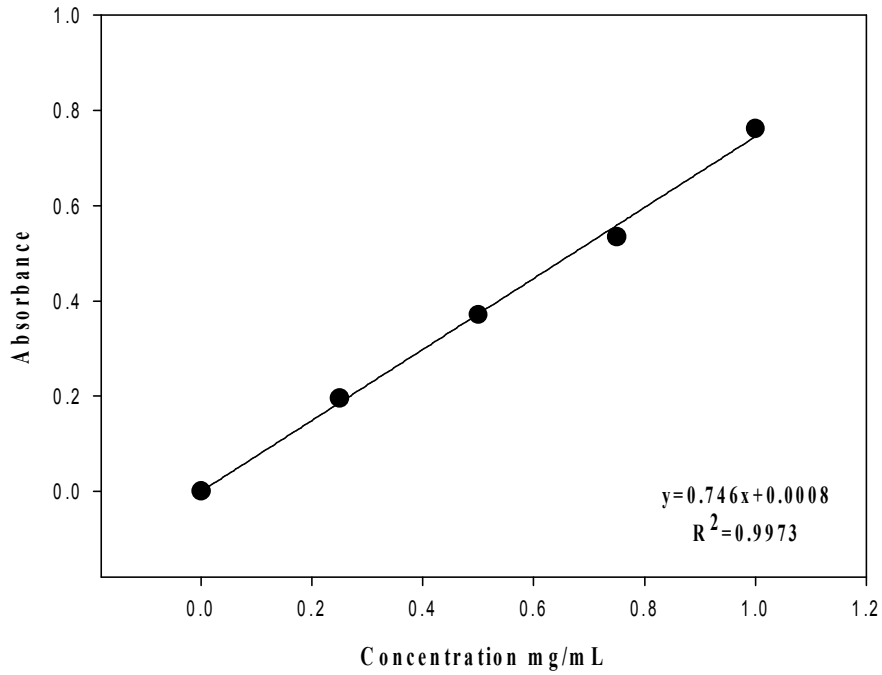

Figure 7. Standard curve for the determination of protein concentration.

7. Enzyme activity assay

GOx oxidized glucose to gluconic acid, accompanied by the formation of hydrogen peroxide, which can oxidize the reduced o-dianisidine in the presence of POD and turn it into the brown red oxidized o-dianisidine. The reaction cocktail solution containing 0.17 mM o-dianisidine and 1.72% D(+)-glucose was prepared immediately before use. The final enzyme assay was determined as reaction cocktail solution 4.99 mL and 600 U/mL POD 10 μL, then the immobilized enzyme was added to start the reaction, and the absorbance value per minute was recorded at 500 nm for 5 minutes.

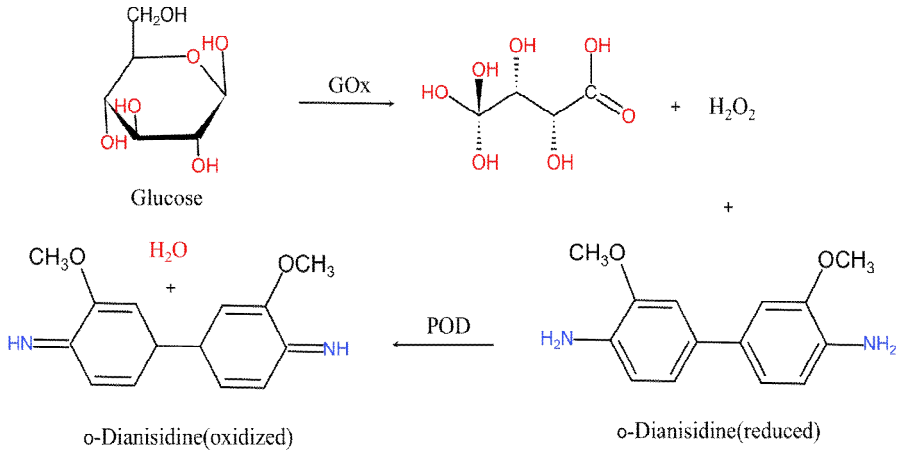

Figure 8. Glucose oxidase is used for the oxidation of glucose and peroxidase is used for the oxidation of o-dianisidine to a stable and colored product for detection.

A colorimetric method was carried out for the determination of LIP activity and stability. LIP activity was determined by hydrolysis of 4-nitrophenyl butyrate at 410 nm. 50 mM 4-nitrophenyl butyrate was prepared in DMF, and the final enzyme assay was to add the immobilized enzyme into 990 μL 20 mM PB buffer solution (pH 6.5), and then 10 μL 4-nitrophenyl butyrate solution was added to start the reaction. The absorbance change within 10 minutes was also measured and recorded [43, 44].

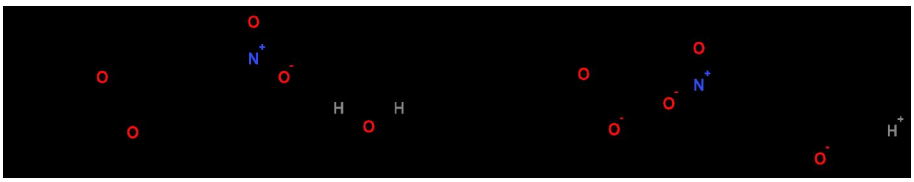

Figure 9. Enzymatic hydrolysis reaction of 4-nitrophenyl butyrate [44].

Table 1. Enzyme activity assay

GOx		LIP	
Reaction cocktail solution : 0.17 mM o-Dianisidine &1.72% D(+)-glucose	4.99 mL	Substrate solution : 50 mM 4-Nitrophenyl butyrate in DMF	10 μL
POD : 600 U/mL	10 μL	20 mM PB (pH 6.5)	990 μL
UV	500 nm	UV	410 nm

8. Storage stability of immobilized enzyme

The immobilized enzyme was stored in the PB buffer solution (pH 7.0) and kept at 4℃. The residual activity of immobilized enzyme was measured periodically for one month, two months. The buffer was used to rinse the foam 1~2 times before each measurement, so as to avoid the effect of the detached immobilized enzyme particles.

9. Application of Micro-PFR with immobilized enzymes

Micro reactor is generally defined as a miniaturized reactor, whose characteristic size is micrometer, and the reaction volume is in the range of nanoliter to microliter [45]. Micro reactors have great improvements in reaction speed, yield, etc. They are safe, reliable, and expandable, enabling a finer process control [46]. The micro reactor selected in this study is a device for chemical reaction in the microchannel. And the reaction system can be divided into a storage portion of a substrate solution, pump (Shimadzu, LC-6AD), micro reactor, and sampling (product out) (Figure 10). The inner diameter and length of PFR are 0.5 cm and 3.5 cm, with the total volume of 690 μL. The voidage of PFR is 87%, so that PFR contains the liquid volume of 600 μL.

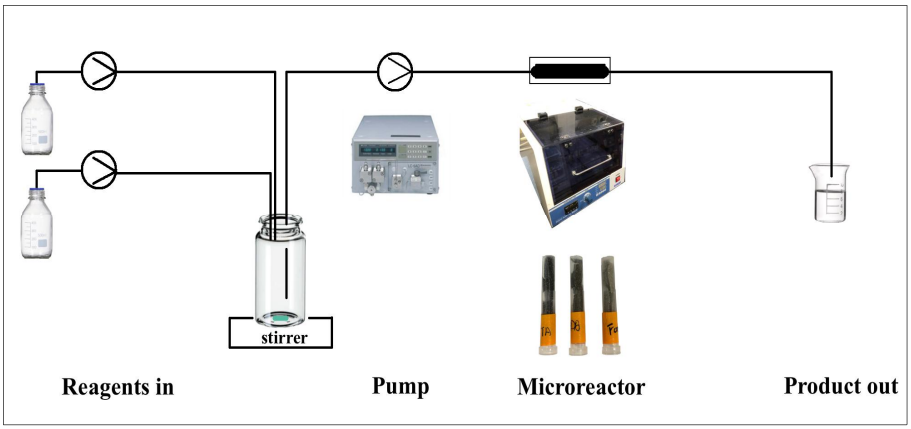

Figure 10. PFR reaction system to detect the stability of immobilized enzyme reactor.

a) Micro-PFR process using immobilized GOx

(1) Production of gluconic acid using Micro-PFR process

In this paper, an easy-to-operate application on micro reactor chromogenic method is used to measure the amount of hydrogen peroxide produced, indirectly indicating the amount of glucose conversion. (Calibration curve as shown in Figure 11)

The substrate solution used in this experiment was 1.72% D(+)-glucose solution, and the reaction was carried out at a flow rate of 5, 4, 3, 2, 1, 0.5 mL/min under the conditions of pH 7.0 and 25℃. 981.72 μL of the solution was collected after the reaction at the outlet. o-Dianisidine 8.28 μL and POD 10 μL were mixed well with a pipette tip, and the absorbance at 500 nm was measured. The results were shown in Figure 12, 13. When the flow rate was set to 1 mL/min, the conversion was relatively high and more profitable, so the stability measurement results were plotted according to the value of 1 mL/min.

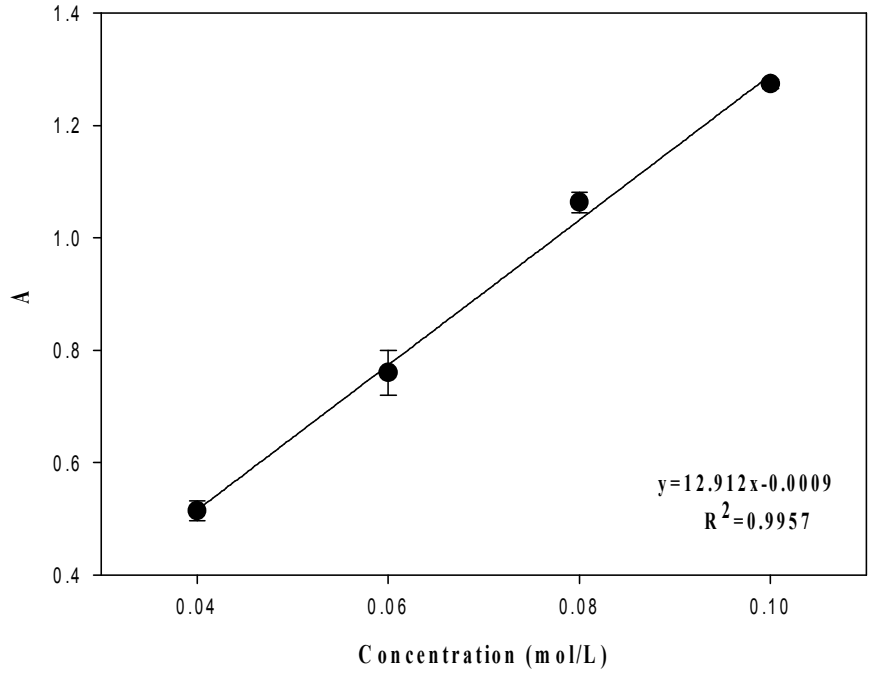

Figure 11. Standard curve for the determination of hydrogen peroxide (H_2O_2) concentration.

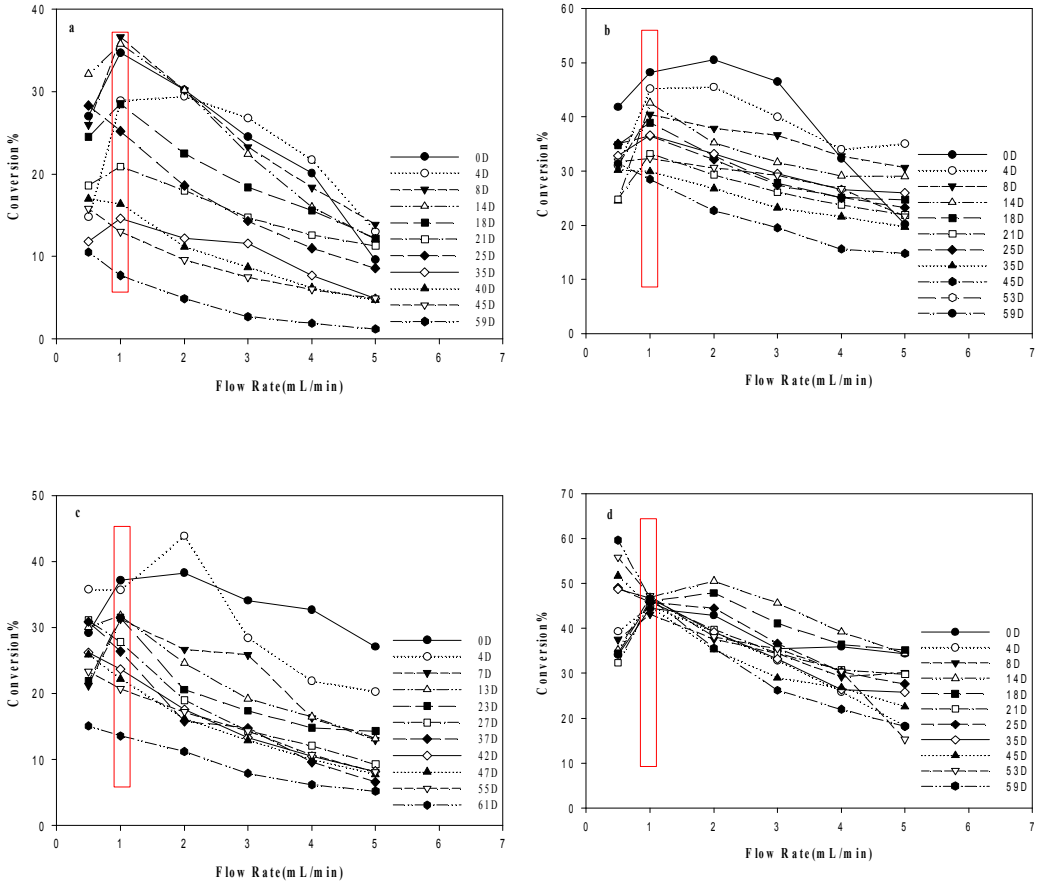

Figure 12. The reaction conversion at the different flow rates. (a) PANI, (b) PAMP, (c) TA@$FeCl_3$__$6H_2O$, (d) PDA.

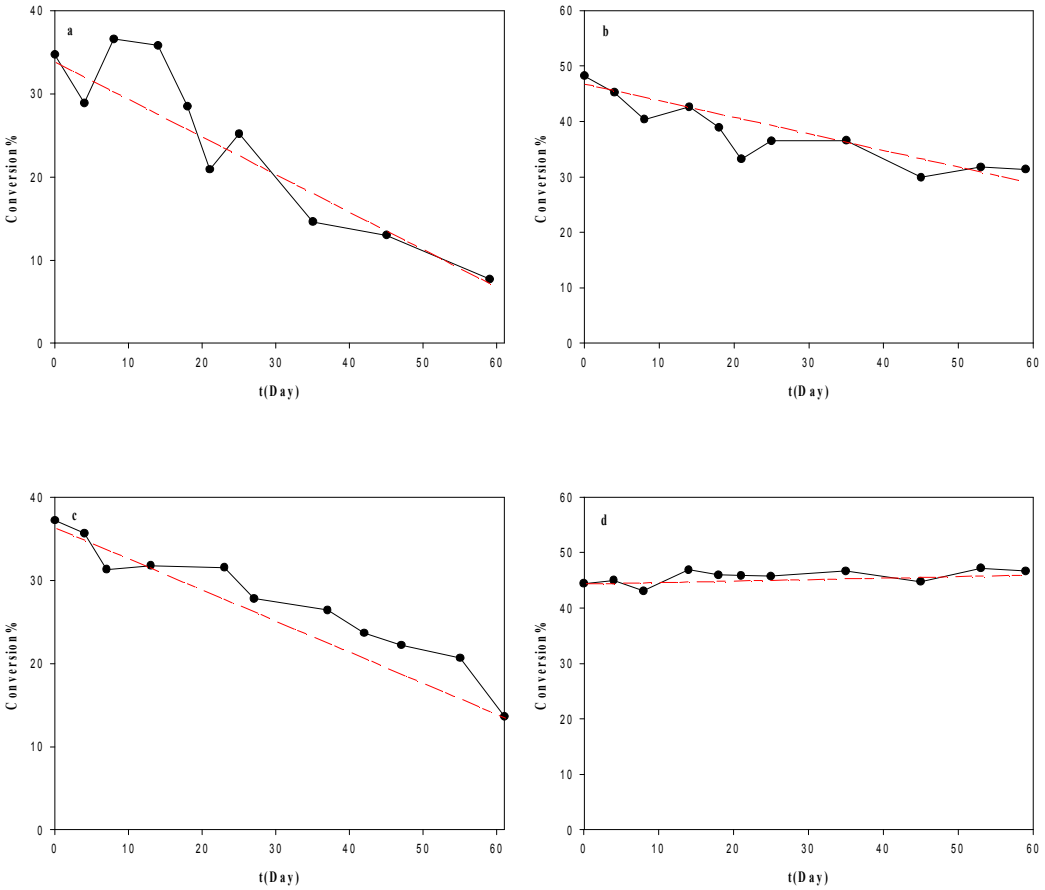

Figure 13. The stability of immobilized GOx at the flow rate of 1 mL/min. (a) PANI, (b) PAMP, (c) TA@$FeCl_3$__$6H_2O$, (d) PDA.

(2) Effect of pH, temperature and substrate concentration on Micro-PFR process

Because most of the enzymes are proteins, their activity is affected by substrate concentration, temperature, pH, factors that destroy protein structure [47]. In the case that the amount of enzyme is constant, there are too many substrates to saturate the enzyme molecule, and the excess substrate molecule cannot react until the substrate has been bound to the enzyme reacts and is released (or released without reacting). Most enzymatic reactions increase in reaction rate with increasing temperature, but at a certain temperature, the protein is denatured due to high temperatures. It is because of the same reason that most enzymes are sensitive to the change of hydrogen ion concentration or pH. Extreme levels of hydrogen ions (high or low) that may denature the enzyme [48]. Any change in pH, even a small one, will change the acidity or basicity of the enzyme and the degree of ionization of the substrate components [49]. And the maximum activity can only be achieved within the optimal pH range.

In this paper, PDA-GOx and PAMP-GOx micro reactor at a flow rate of 1 mL/min were used as research objects to study the effects of substrate concentration, temperature, and pH value on glucose conversion. In order to reduce the experimental error, samples were taken after 30 minutes of system operation. In the range of glucose concentration 1.72~5.72%, temperature 25~65℃, pH 4~8, the optimum of substrate concentration, temperature, and pH was determined. As can be seen from Figure 14, when the glucose concentration was higher, the reaction reached saturation state and the efficiency of conversion was lower, so the glucose with a concentration of 1.72% was selected for subsequent experiments. What is more, as can be seen from Figure 15 that the highest conversion of PDA-GOx occured at 35℃, pH 5, and the highest conversion of PAMP-GOx occured at 35℃, pH 6.

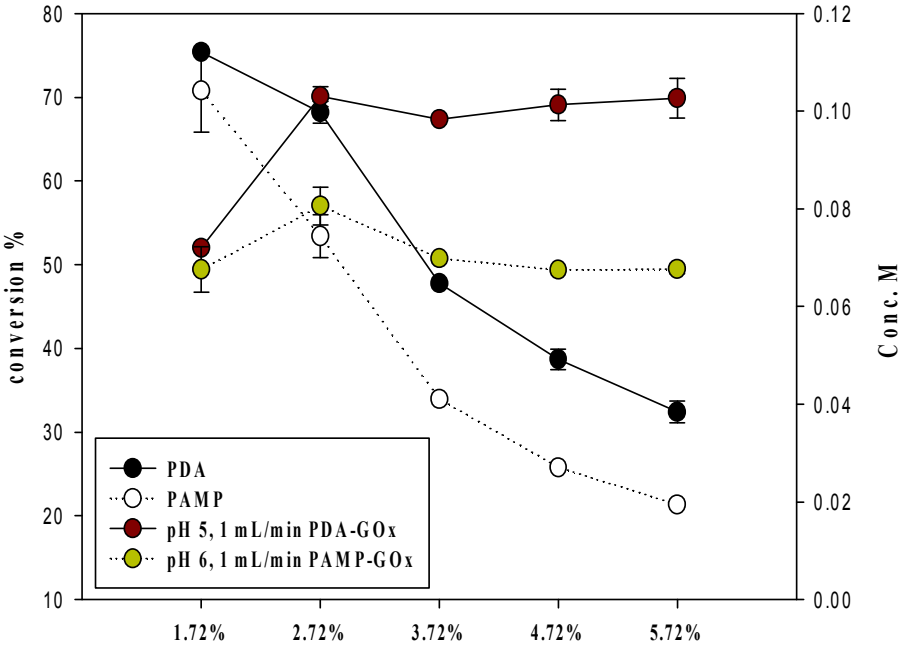

Figure 14. Effect of feed glucose concentration on yield. (at 25℃, 1 mL/min)

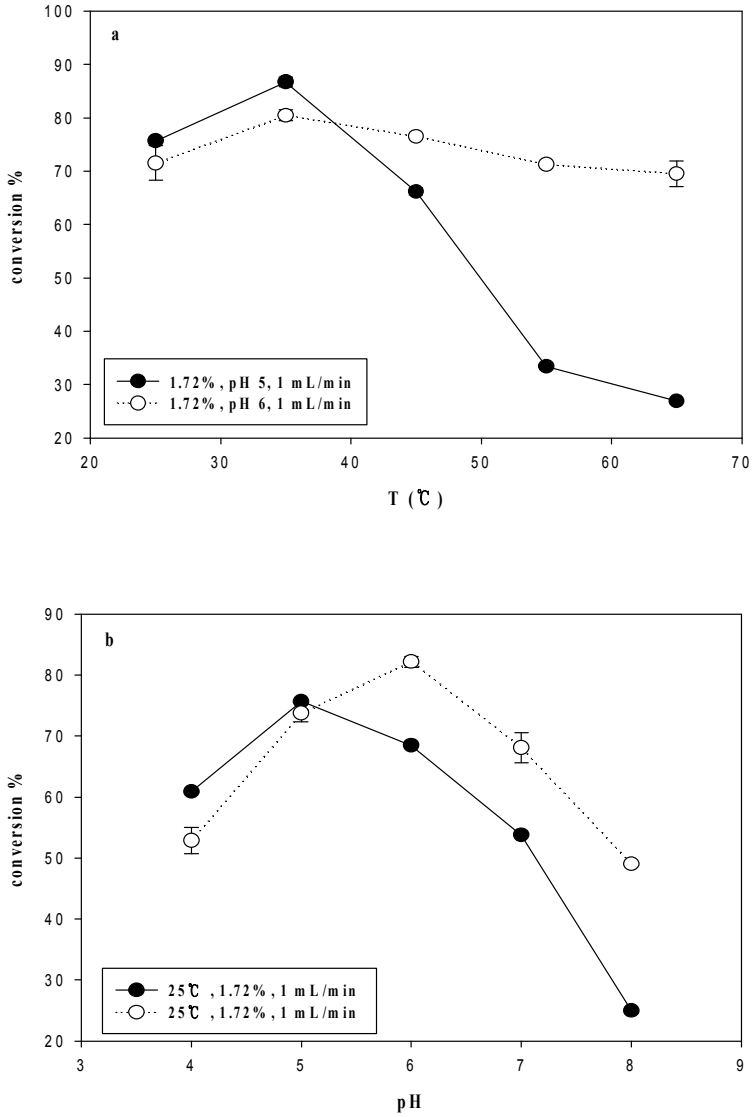

Figure 15. Effect of a. temperature, and b. pH on gluconic acid yield. (● PDA-GOx, ○PAMP-GOx)

(3) Response surface analysis of Micro-PFR

The Response Surface Methodology (RSM) is a widely used mathematical and statistical method for modeling and analyzing processes with the goal of optimizing responses [50], especially if is affected by several variables, due to its low computational effort. The advantage of RSM is to establish interactions between variables, together with mathematical models, and reduce the number of experiments, so saving time and costs [51]. It is mainly carried out in the following three steps. The first one is a screening test that helps select the key factors that are expected to affect the response. Secondly, the experiment is performed by using a central integrated design of two variables or a Box-Behnken design method of three variables under optimal conditions, and the optimal conditions for optimizing the variables of the response values in the target region are searched. The final step is to verify the importance of the model formed in the response surface analysis and the repeatability by comparing the actual experimental values with the expected response values after actual experiments under optimized conditions [52, 53].

In this experiment, response surface analysis of PDA-GOx and PAMP-GOx was performed by pH and temperature of the independent factors affecting gluconic acid conversion. According to the measurement results of the independent factor (Figure 15), PDA-GOx was centered at 35°C and pH 5, and PAMP-GOx was designed with 35°C and pH 6 as the center point to obtain optimal conditions.

As seen from Table 2, the Model F-value of 122.18 implies the model is significant. There is only a 0.01% chance that an F-value this large could occur due to noise. In this case, temperature, pH, there interactions are all significant terms. The "Pred R-Squared" of 0.9194 is in reasonable agreement with the "Adj R-Squared" of 0.9806; i.e. the difference is less than 0.2. "Adeq Precision" that measures the signal to noise ratio. A ratio greater than 4 is desirable while the ratio of 24.035 indicates an adequate signal. This model can be used to navigate the design space. The final optimal operating conditions for PDA-GOx Micro-PFR were temperature 29.5°C, pH 5.25.

The same can be seen from Table 3, the Model F-value of 44.86 implies the model

is significant. There is only a 0.01% chance that an F-value this large could occur due to noise. In this case, pH, temperature and pH interaction are significant terms. But the factor temperature is not significant. The "Pred R-Squared" of 0.8137 is in reasonable agreement with the "Adj R-Squared" of 0.9481; i.e. the difference is less than 0.2. "Adeq Precision" measures the signal to noise ratio. A ratio greater than 4 is desirable. The ratio of 15.944 indicates an adequate signal. This model can be used to navigate the design space. The final optimal operating conditions for PAMP-GOx Micro-PFR were temperature 31.8°C, pH 6.31.

Table 2. ANOVA for Response Surface Quadratic model of PDA-GOx

Source	Sum of Squares	df	Mean Square	F Value	p-value
Model	9408.80	5	1881.76	122.18	< 0.0001
A-pH	94.23	1	94.23	6.12	0.0426
B-T	393.43	1	393.43	25.55	0.0015
AB	220.52	1	220.52	14.32	0.0069
A^2	5444.18	1	5444.18	53.49	< 0.0001
B^2	4382.68	1	4382.68	284.57	< 0.000
Residual	107.81	7	15.40		
Lack of Fit	107.81	3	35.94		
Pure Error	0.000	4	0.000		
Cor Total	9516.61	12			

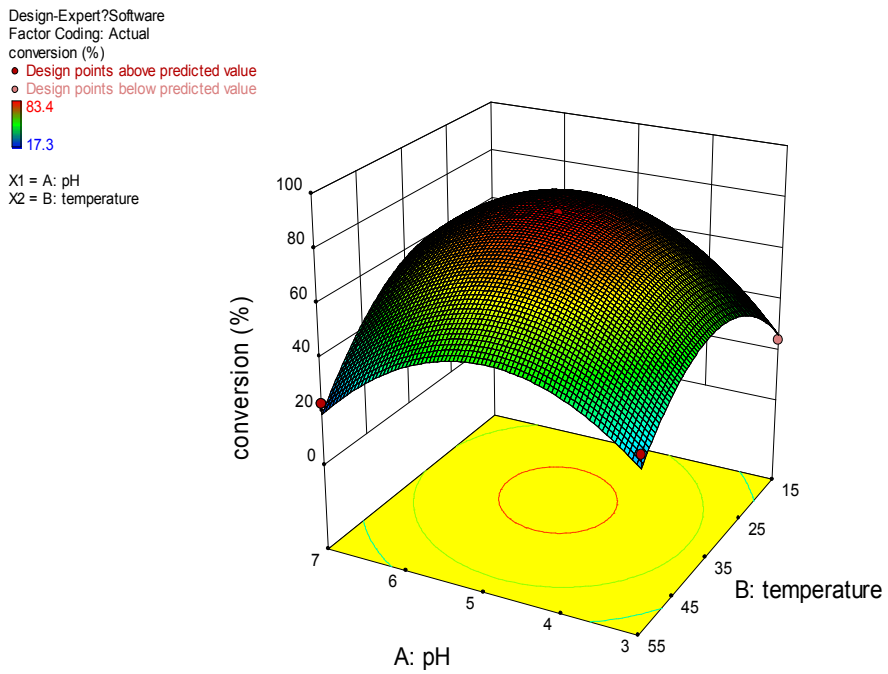

Figure 16. Response surface graph of gluconic acid yield (%) with temperature and pH. (PDA-GOx)

Table 3. ANOVA for Response Surface Quadratic model of PAMP-GOx

Source	Sum of Squares	df	Mean Square	F Value	p-value
Model	3746.65	5	749.33	44.86	< 0.0001
A-pH	98.38	1	98.38	5.89	0.0456
B-T	11.17	1	11.17	0.67	0.4405
AB	694.32	1	694.32	41.56	0.0004
A^2	2187.31	1	2187.31	130.94	< 0.0001
B^2	527.74	1	527.74	31.59	0.0008
Residual	116.94	7	16.71		
Lack of Fit	116.94	3	38.98		
Pure Error	0.000	4	0.000		
Cor Total	3863.58	12			

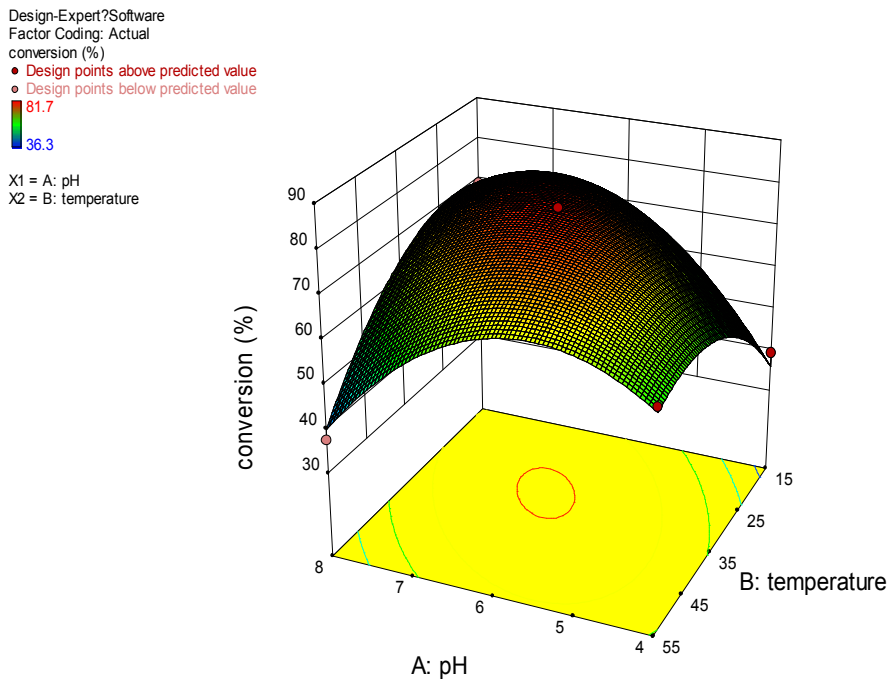

Figure 17. Response surface graph of gluconic acid yield (%) with temperature and pH. (PAMP-GOx)

(4) Study on the operational stability of immobilized enzymes with Micro-PFR

Living organisms use various enzymes in their bodies to synthesize necessary substances break down and sustain life. The decomposition or synthesis reactions are all performed at room temperature and atmospheric pressure, effectively producing what is suitable for our body. Realizing this process in a living body to an external device can produce an ideal production that makes it easier to achieve resource and energy saving. The reaction device with this principle used is called a bioreactor. Bioreactors perform biochemical reactions by adding biocatalysts and substrates to economically produce the desired substances, and there are measurement and control devices to make biochemical reactions efficiently perform under optimal conditions. Considerations for designing bioreactors include increasing the rate of substrate conversion to product, product concentration and yield, productivity and stability, and for continuous reactions, enzymatic immobilization methods that can be used without long-term replacements. In addition, unlike other catalysts, enzymes work only on specific reactions, which do not produce unnecessary substances.

The PFR reactor with the total volume of 600 μL was operated under the optimal reaction conditions obtained in the previous step. And the condition had been set to glucose concentration was 1.72%, and the flow rate was 1 mL/min.

b) Micro-PFR process using immobilized LIP

LIPs are enzymes based on ester bonds, whether they are hydrolyzed or synthesized, depending on the water in the reaction medium. Because of the stability in organic solvents, wide substrate specificity, stereoselectivity and regioselectivity, they are important biocatalysts for various biotechnological applications [54]. LIP is also a catalyst that can be used in large quantities at an industrial level. In order to obtain maximum yield in a biological process, the variable stability of the enzyme in the reactor is detected [44]. 4-NPB was selected as the reaction substrate, and its operational stability was measured by measuring the conversion of 4-nitrophenolate anion (Figure 18) released by the reaction. It can be seen from Figure 19 that the conversion of LIP immobilized on TA@$FeCl_3$_$6H_2O$ and PDA was 95.5% and 97.7% respectively in the retention time of 3 minutes, while the conversion of PANI and PAMP immobilized lipase was only 78.4% and 89.1% at the same retention time. Therefore, TA@$FeCl_3$_$6H_2O$ and PDA immobilized LIP were selected to determine the operational stability of the Micro-PFR.

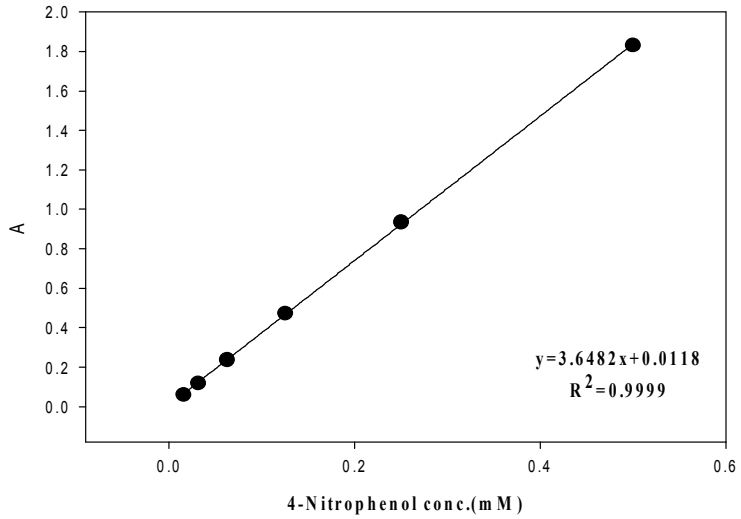

Figure 18. Standard curve for the determination of 4-nitrophenol concentration. (pH 6.5)

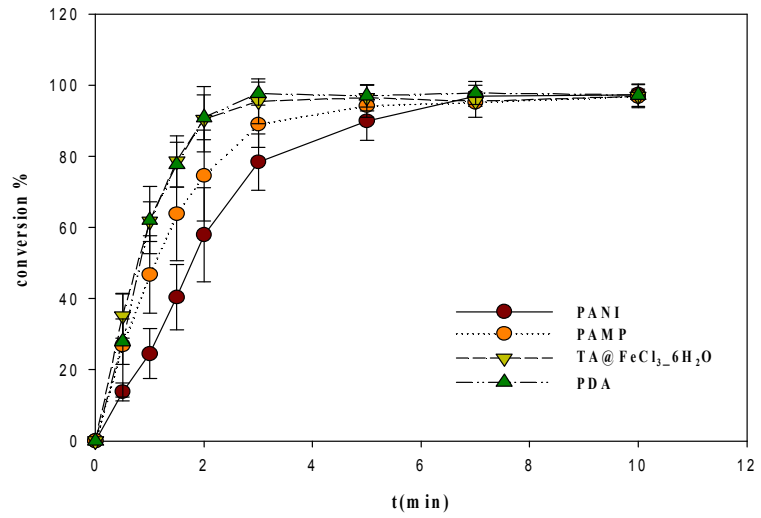

Figure 19. 4-Nitrophenolate conversion using Micro-PFR.

III. Results and Discussion

A. Morphology and size of immobilized GOx/LIP

The surface morphology of the carrier materials before and after immobilization was observed by scanning electron microscope, with the image shown in Figure 20. It can be seen from Figure 20 (a) that the surface of the Ni-foam was very smooth and flat, so that the space available for immobilization of the enzyme was limited and not easy to adhere. Figure 20 (d, g, j, m) was the composite material of the coating on the surface of the Ni-foam. Physically, the stereoscopic space on the surface of the Ni-foam was increased, providing a larger surface area for enzyme attachment. In the chemical sense, the polyaniline material can offer an amino group, TA@$FeCl_3$_$6H_2O$ a hydroxyl group, and PDA has both a hydroxyl group and an amino group. The group makes the covalent bond formed by immobilization of the enzyme more stable. Observing Figure 20 (d, g), PANI and PAMP showed a bar shape with a length between 150 and 200 nm. Using the synthesis method in this experiment, the generated PANI and PAMP were shorter. Compared with other studies, it is more accurate to define nano rod-shaped structure than nano fiber-shaped structure. Figure 20 (j) showed that TA@$FeCl_3$_$6H_2O$ synthesized by the method derived from Hirotaka Ejima *et al*. was a sphere with a diameter of 40 nm and Figure 20 (m) showed that PDA was an irregular spherical micro particle with a diameter between 0.3 and 0.6 μm, while the study of Guohua Jiang *et al*. [Ref] showed that PDA particle under slight vibration was a shape gauge. The results showed that the morphology of PDA in this study was changed after the vigrous during PDA coating. Moreover, Figure 20 (b, e, h, k, n) was the morphology changes after GOx immobilization. From these results, it can be clearly seen that the surface was attached with a layer of granular substance. Figure 20 (c, f, i, l, o) was the morphology changes after LIP immobilization. The LIP was immobilized on the polyaniline material to form a crystalline substance. The immobilized LIP on PANI, decreased immobilization efficiency and reduced the enzyme activity.

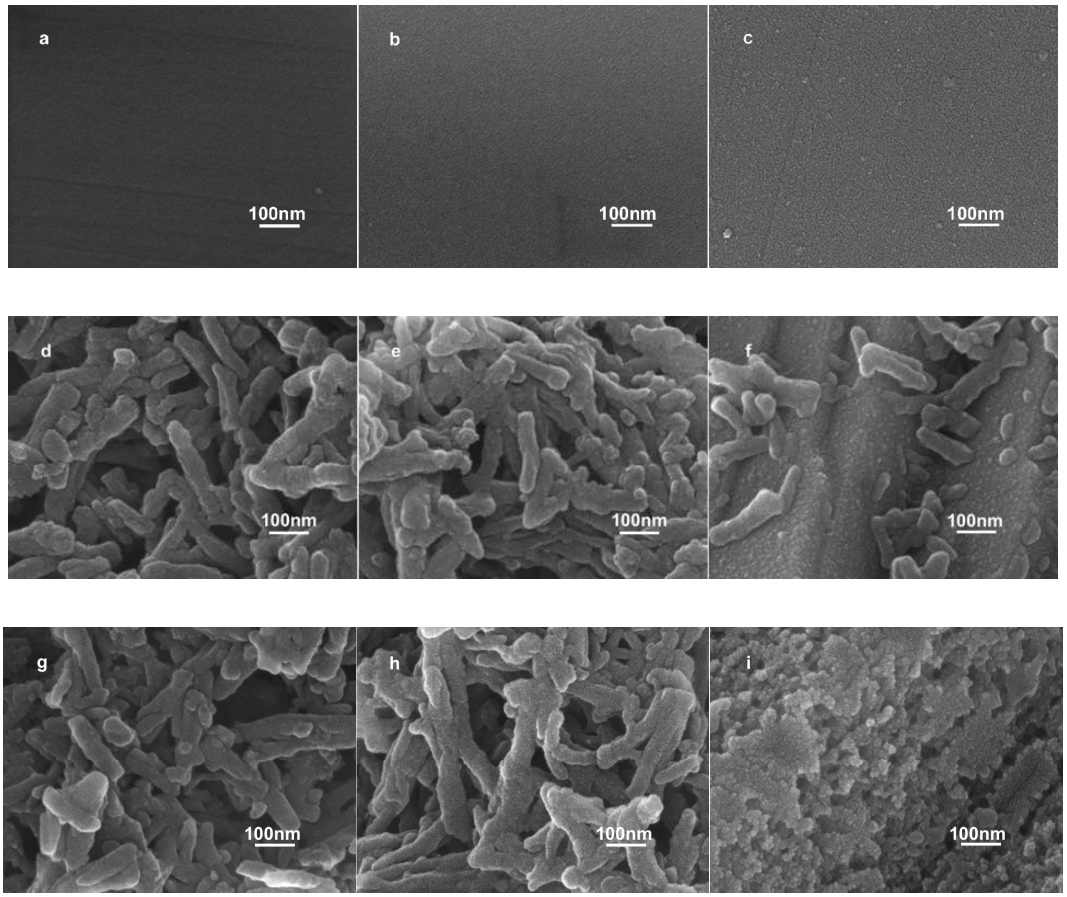

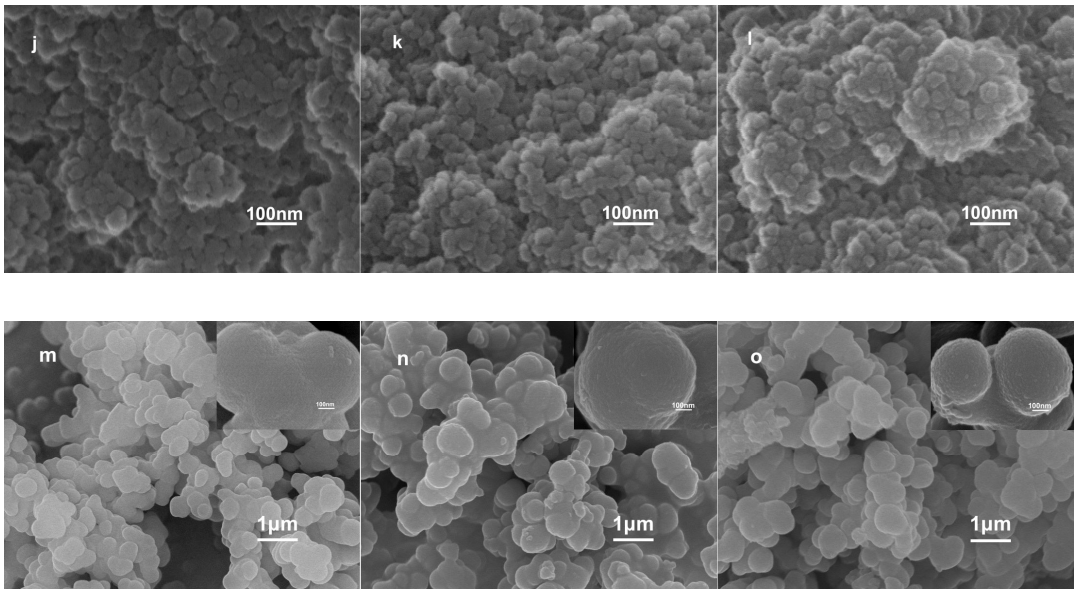

Figure 20. SEM images of (a) Ni-foam, (b) Ni-foam-GOx, (c) Ni-foam-LIP, (d) Ni-foam-PANI, (e) PANI-GOx, (f) PANI-LIP, (g) Ni-foam-PAMP, (h) PAMP-GOx, (i) PAMP-LIP, (j) Ni-foam-TA@$FeCl_3$_$6H_2O$, (k) TA@$FeCl_3$_$6H_2O$-GOx, (l) TA@$FeCl_3$_$6H_2O$-LIP, (m) Ni-foam-PDA, (n) PDA-GOx, (o) PDA-LIP.

B. Surface chemistry analysis

The FTIR spectrum provides direct evidence for the synthesis of various polymeric materials (Figure 21-23). As shown in Figure 21, the absorption peaks at 1578 cm^{-1} and 1489 cm^{-1} were attributable to the C=C stretching of the quinoid and the benzene rings, indicating the oxidation state of emeraldine salt of PANI. For PANI, the peaks at 1292 cm^{-1} and 1240 cm^{-1} (for PAMP, the peaks at 1296 cm^{-1} and 1242 cm^{-1}. the peak shifting can be due to bond formation between Fe_3O_4 and polyaniline) were attributed to the bending vibration of C-N to aromatic amine/imine and the stretching vibration of C-N in polarized structure. And the peak at 1128 cm^{-1} was attributed to the aromatic C-H in-plane bending vibration, which was often related to the doped structure indicating the presence of protonated conductive PANI induced by acid doped polymer. The observed bands at 878 cm^{-1}, 769 cm^{-1} and 690 cm^{-1} can be assigned to the aromatic ring. The out-of-plane deformation vibration of the C-H bond in the benzene ring and the distributed aromatic ring indicated the formation of the polymer [55-59]. And the pure Fe_3O_4 spectrum showed Fe-O-Fe stretching vibration at 675 cm^{-1}. Compared with the three spectra, PAMP had a relatively broad characteristic peak at this position, which proved that our synthesized magnetic nanoparticles were based on PANI [60, 61].

The FTIR spectrum of tannic acid and TA@$FeCl_3$_$6H_2O$ complex was shown in Figure 3. For tannic acid (as shown in Figure 22), the broad band in the range of 3500~3000 cm^{-1} was hydrogen bond OH tensile vibration, and the peak at 1704 cm^{-1} was attributed to the C=C bond on the benzene ring, along with the peak between 1608 cm^{-1} and 1083 cm^{-1}. Due to the C-C tensile vibration, C-H bond on the benzene ring, and the stretching of the C-O band, the peaks at 1083 cm^{-1} and 1022 cm^{-1} belonged to O-H of phenolic. Compared with the three spectra, namely the peak of TA@$FeCl_3$_$6H_2O$ at the same position as the characteristic peak of $FeCl_3$_$6H_2O$, TA@$FeCl_3$_$6H_2O$ was wider than the tannic acid peak, which proved that the synthesized complex was formed by chelation of tannic acid with iron ions [62-64].

The FTIR spectrum of dopamine and PDA was shown in Figure 23. And the spec-

trum of dopamine showed characteristic peaks at 3034 cm^{-1} and 2956 cm^{-1}, which were attributed to the aromatic O-H stretching vibrations. Then arrow peaks at 1319 cm^{-1}, 1188 cm^{-1}, and 1174 cm^{-1} were attributed to the C-O-H bending vibration, C-O symmetry vibration, and C-C stretching vibration modes, respectively. The sharp peaks at 1498 cm^{-1} and 1471 cm^{-1} were corresponding to the stretching vibrations of benzene ring. For PDA, it was apparent that a broad strong peak appears at 3500~3000 cm^{-1} in the spectrum, which is attributed to the stretching vibration of N-H and O-H. And the vibration peaks at 1558 cm^{-1} and 1506 cm^{-1} were components of indole aromatic C=C bonds and C=N bonds, the vibration peak at 1282 cm^{-1} the tensile vibration of C-O-H on the benzene rings, and at 1118 cm^{-1} the shear vibration of C-O. Thus it can be confirmed that the synthesized polymer was PDA [65, 66].

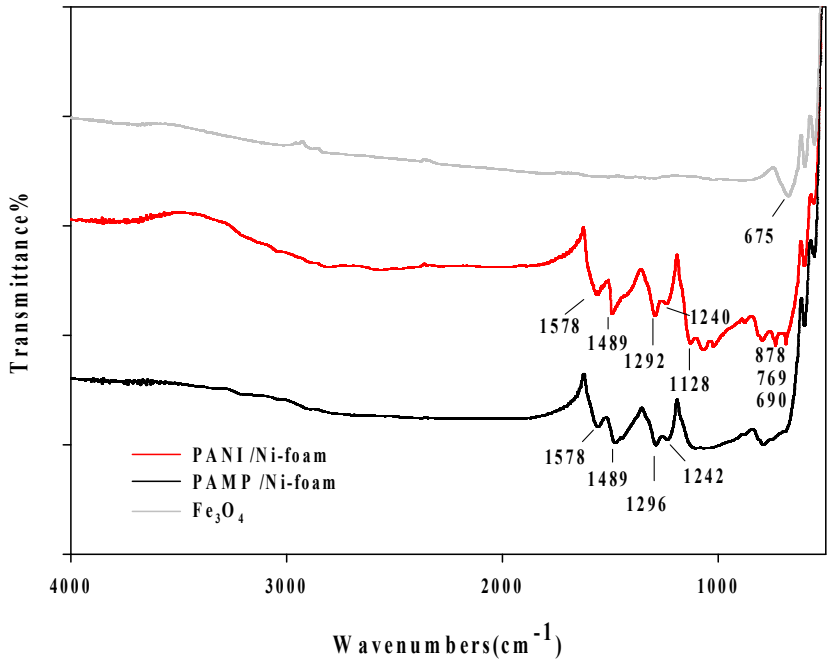

Figure 21. FTIR-ATR spectra of PANI/Ni-foam, PAMP/Ni-foam and Fe_3O_4.

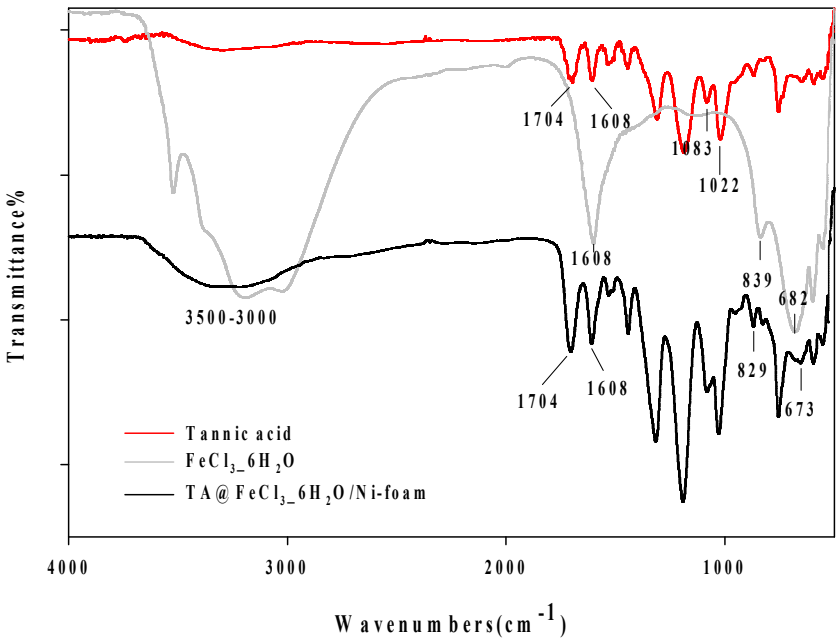

Figure 22. FTIR-ATR spectra of tannic acid, $FeCl_3$_$6H_2O$ and TA@$FeCl_3$__$6H_2O$/Ni-foam.

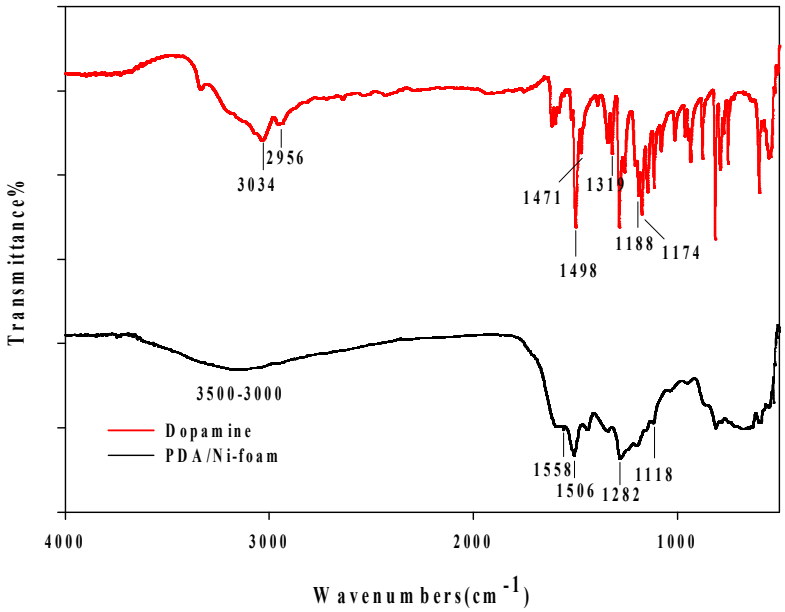

Figure 23. FTIR-ATR spectra of dopamine and PDA/Ni-foam.

C. Enzyme loading analysis

The stability of immobilized enzyme was changed with enzyme loading and immobilization yield [67]. The immobilization yield was measured using 2 mg/mL enzyme solution. Table 4 showed the immobilization yields of GOx/LIP onto different carriers. The amount of immobilized enzyme on the coated Ni-foam was increased more than 70%, compared to that with bare Ni-foam. Although LIP immobilized on the PANI coated Ni-foam was the highest, it was found that the enzyme activity was not good.

Table 4. The immobilization yield of enzyme onto different carriers (≤±5%)

Enzyme	Carriers				
	Ni-foam	PANI	PAMP	TA@$FeCl_3$_6 H_2O	PDA
Glucose oxidase	67.20%	78.98%	75.60%	75.70%	75.90%
Lipase	52.30%	85.00%	73.20%	79.5%	72.10%

D. Storage stability analysis

Immobilization of enzymes on a proper material can increase the rigidity of enzyme, and thus improves the stability under operational conditions by preventing conformational changes [68]. As shown in Figure 24 (a), the activity of GOx immobilized on the synthetic particles coated on the surface of Ni-foam is significantly stronger than that of bare Ni-foam. The activity of GOx immobilized Ni-foam almost disappeared after a month. However, the residual activities of PANI, PAMP, TA@$FeCl_3$_$6H_2O$, PDA were 50.9%, 70.4%, 72.1%, 73.4%, respectively. Generally speaking, the modified Ni-foam as immobilization carrier material significantly improved the activity of immobilized enzyme than the bare Ni-foam. Though its stability is not measured under the optimal conditions, it still has high activity after one month.

Figure 24 (b), the activity of LIP immobilized on uncoated Ni-foam was higher than that of PAMP, PANI, PDA coatings, but the stability was not good. Immobilized LIPs on TA@$FeCl_3$_$6H_2O$ was the most stable and had the best residual enzyme activity, followed by PDA, PAMP, which were 82.6% and 71.2% of TA@$FeCl_3$_$6H_2O$ immobilized enzyme. For LIP immobilized on PANI, the enzyme activity was low. From the SEM images, it can be seen that PANI formed crystal after immobilization process, changed its original shape, and reduced the spatiality. The structure of the enzyme changed because of the formation of crystallization. And the active center of the enzyme was covered, leading to the inactivation of enzymes. And the results of repeated experiments were all the same. After a month, the residual activities of enzyme immobilized on bare Ni-foam, PANI, PAMP, TA@$FeCl_3$_$6H_2O$, and PDA were 83.1%, 73.3%, 93.4%, 90.1%, and 98.3%, respectively. As we know, LIP shows a typical mechanism of action called interfacial activation, in aqueous media the active site is protected by an oligopeptide chain known as “lid” [69]. Therefore, the stability of LIP itself is better than that of GOx. In addition, the suitable carrier materials make the stability of LIP reach 2 months, 6 months or even more than one year.

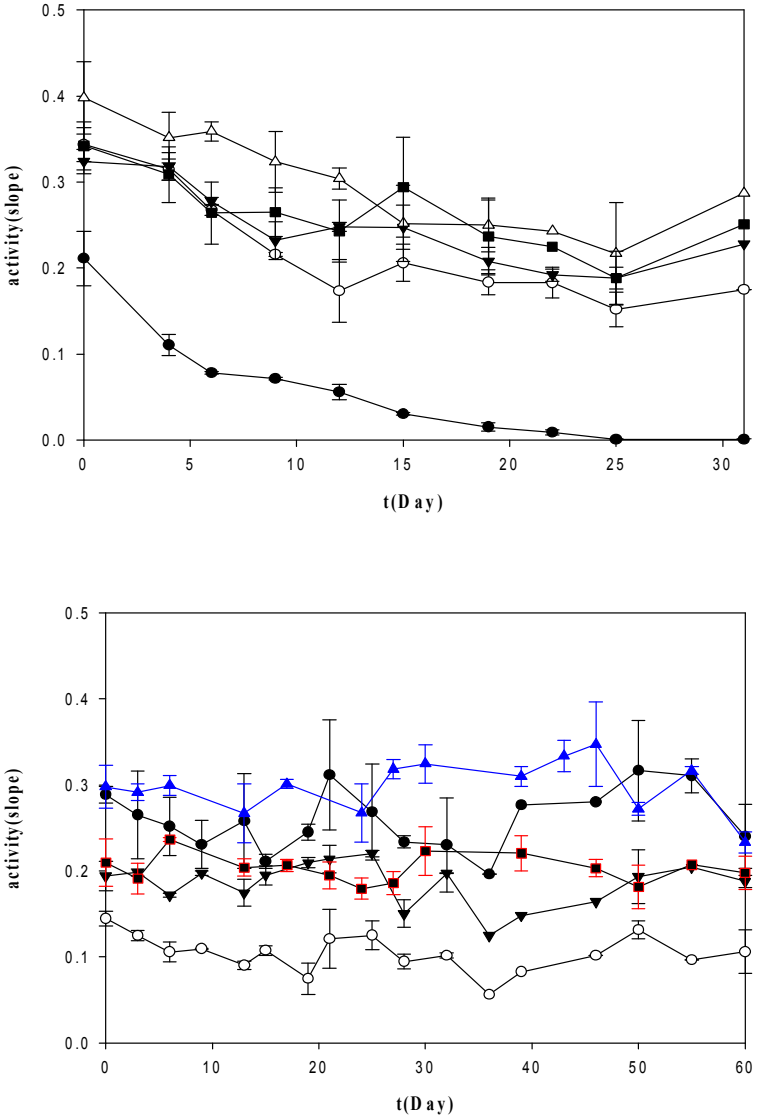

Figure 24. Storage stabilities of immobilized (a) GOx, (b) LIP 2 mg/mL at 4℃. (● Ni−foam, ○ PANI, ▼ PAMP, △ TA@$FeCl_3$_$6H_2O$, ■ PDA)

E. Stability analysis of Micro-PFR

1. Operational stability of immobilized GOx

In this experiment, the immobilized enzyme of PDA-GOx and PAMP-GOx were selected to run Micro-PFR under the optimal temperature and pH to obtain the highest gluconic acid conversion. The enzyme operational stability as shown in Figure 25 was carried out with the method described in the section Ⅱ-B-9-a). The glucose conversion of PDA-GOx decreased from 84.6±4.7% to 18.4±2.3% after 172 hours of continuous operation, while that of PAMP-GOx decreased from 82.1±1% to 22.2±4.4%.

A study has shown that after 8 times of repetitive uses, 60% of the enzyme activity remains, which leads to the conclusion that the enzyme has high stability and reusability [68]. In this paper, the activity of the immobilized GOx reactor is still stable after 24 hours continuous operation. The conversion maintained over 80% for 24 hours reaction, provided high activity.

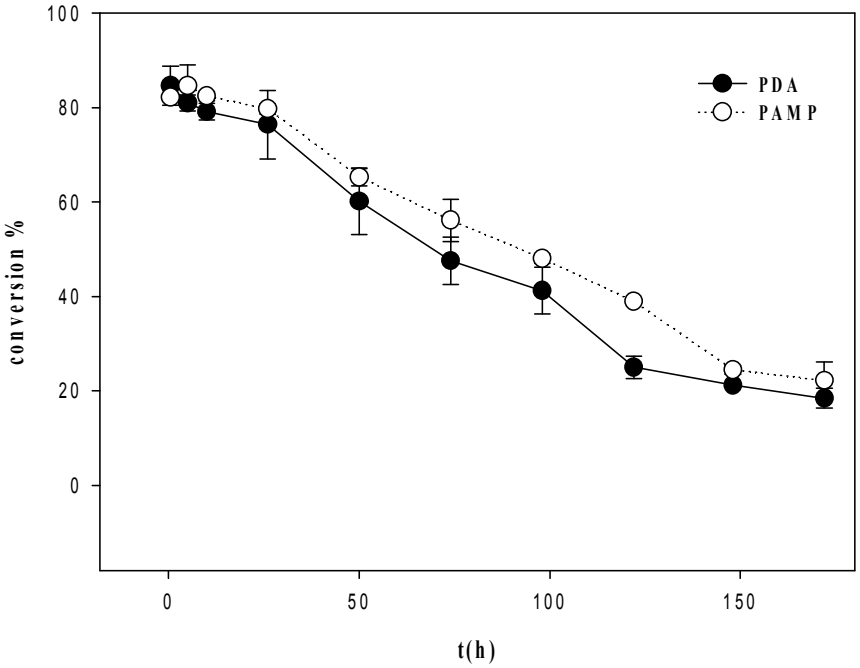

Figure 25. The operational stability of the immobilized GOx in a Micro-PFR under optimal conditions.

2. Operational stability of immobilized LIP

According to Figure 19, the activity of TA@$FeCl_3$_$6H_2O$-LIP and PDA-LIP was higher than PANI-LIP and PAMP-LIP. When the retention time was 3 minutes, the conversion increased over 95%. The conversion with PANI-LIP reached 95% at the retention time of 7 minutes, and that with PAMP-LIP reached 95% at the retention time of 5 minutes. Therefore, TA@$FeCl_3$_$6H_2O$-LIP and PDA-LIP were selected as appropriate immobilized enzymes for continuous operation. With the retention time of 3 minutes, the operation stability of the Micro-PFR was measured and shown in Figure 26.

The conversion of PDA-LIP decreased from 96.9±2.3% to 95.8±3%, and that of TA@$FeCl_3$_$6H_2O$-LIP decreased from 95.3±3.63% to 94.3±4.37% after 24 days continuous operation.

Similarly, the application stability of immobilized LIP in the reactor was more expressed by measuring the cycles of reaction. In this experiment, its stability was expressed by continuously measuring its reaction activity. It can be seen that after 24 days of measurement, the enzyme activity was reduced slightly, the conversion was still over 90%, and the stability was excellent.

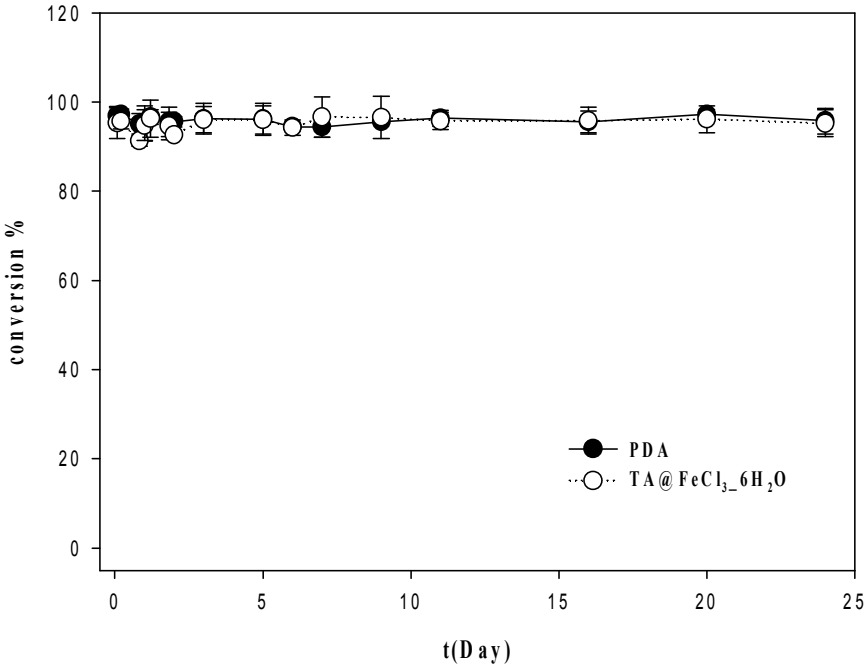

Figure 26. The operational stability of the immobilized LIP in a Micro-PFR at pH 6.5 and room temperature.

IV. Conclusion

The development of immobilization technology improves the stability and reusability of enzyme. In the process of immobilization, the selection of carriers is the key step, whose structure and performance will have a great impact on the enzymatic properties of immobilized enzyme. Appropriate and excellent carriers provide functional groups and higher surface area for enzyme immobilization and show higher enzyme activity. In this paper, Ni-foam, which is cheap, easy to operate and easy to separate from the reaction solution, is used as the basic carrier material. PANI, PAMP, TA@$FeCl_3$_$6H_2O$ and PDA are used to modify the surface of the Ni-foam in order to study the effect of the Ni-foam on the stability of immobilized GOx and LIP. A micro PFR reactor, is developed to test the operational stability of the immobilized enzyme. After a series of measurements, the following conclusions are drawn:

(1) Since the surface of Ni-foam is smooth, and the activity and stability is very low and easy to detach from the surface. The nickel foam modified with coating has both abundant enzyme attachment point and spatial structure, which greatly increases the immobilization efficiency amd stability of enzyme.

(2) For GOx, the immobilized enzyme on the coated Ni-foam was 1.5~2 times higher than that on the Ni-foam directly. After a month, the residual activity of PANI, PAMP, TA@$FeCl_3$_$6H_2O$, PDA accounted for 50.9%, 70.4%, 72.1%, 73.4%, respectively. For LIP, the activity of LIP immobilized on uncoated Ni-foam was higher than that of PAMP, TA@$FeCl_3$_$6H_2O$, PANI, PDA coatings, but the stability was not good. It was stable on TA@$FeCl_3$_$6H_2O$ and had the best residual enzyme activity, followed by PDA, PAMP. After one month, the residual activities of enzyme immobilized on PANI, PAMP, TA@$FeCl_3$_$6H_2O$, and PDA were 83.1%, 73.3%, 93.4%, 90.1%, and 98.3%, respectively. For the LIP immobilized on PANI, the enzyme activity was low. From the SEM images, it can be seen that PANI formed crystal after immobilization process, changed its original shape, and reduced the surface area.

(3) The stability of the GOx and LIP used was higher than that of the previous immobilized enzyme and used for the development of enzyme conversion process. The

micro plug flow reactor with two immobilized enzymes showed increased the operational stability. The conversions of PDA-GOx decreased from 84.6±4.7% to 18.4±2.3%, while that of PAMP-GOx decreased from 82.1±0.4% to 22.2±4.4% after 172 hours of continuous operation. The conversions of TA@$FeCl_3$_$6H_2O$-LIP and TA@$FeCl_3$_$6H_2O$-LIP were over 90% after 24 days operation.

(4) In summary, the PDA coated Ni-foam is also suitable for the immobilization of GOx and LIP, possible due to the fact that its surface has both -NH and -OH functional groups.

References

[1]Zdarta, J., et al., A general overview of support materials for enzyme immobilization: characteristics, properties, practical utility. Catalysts, 2018. 8(2): p. 92.

[2]Homaei, A.A., et al., Enzyme immobilization: an update. Journal of Chemical Biology, 2013. 6(4): p. 185-205.

[3]Tosa, T., et al., Studies on continuous enzyme reactions. I. Screening of carriers for preparation of water-insoluble aminoacylase. Enzymologia, 1966. 31(4): p. 214.

[4]Datta, S., L.R. Christena, and Y.R.S. Rajaram, Enzyme immobilization: an overview on techniques and support materials. 3 Biotech, 2013. 3(1): p. 1-9.

[5]Nguyen, H.H. and M. Kim, An overview of techniques in enzyme immobilization. Applied Science and Convergence Technology, 2017. 26(6): p. 157-163.

[6]Jesionowski, T., J. Zdarta, and B. Krajewska, Enzyme immobilization by adsorption: A review. Adsorption, 2014. 20(5-6): p. 801-821.

[7]Ke, C., et al., Recent advances in enzyme immobilization. Sheng Wu Gong Cheng Xue Bao= Chinese Journal of Biotechnology, 2018. 34(2): p. 188-203.

[8]Tischer, W. and F. Wedekind, Immobilized enzymes: methods and applications, in biocatalysis-from discovery to application. 1999, Springer. p. 95-126.

[9]Brady, D. and J. Jordaan, Advances in enzyme immobilisation. Biotechnology Letters, 2009. 31(11): p. 1639.

[10]Barbosa, O., et al., Glutaraldehyde in bio-catalysts design: A useful crosslinker and a versatile tool in enzyme immobilization. Rsc Advances, 2014. 4(4): p. 1583-1600.

[11]Satar, R., et al., Role of glutaraldehyde in imparting stability to immobilized β -galactosidase systems. Brazilian Archives of Biology and Technology, 2017. 60.

[12]Yang, H. and Y. Zhu, Size dependence of SiO_2 particles enhanced glucose biosensor. Talanta, 2006. 68(3): p. 569-574.

[13]Weidenbach, G., D. Bonse, and G. Richter, Glucose isomerase immobilized on SiO_2 -carrier with high productivity. Starch-Starke, 1984. 36(12): p. 412-416.

[14]Chang, Q. and H. Tang, Immobilization of horseradish peroxidase on NH_2-modified magnetic Fe_3O_4/SiO_2 particles and its application in removal of 2, 4-dichlorophenol. Molecules, 2014. 19(10): p. 15768-15782.

[15]Rani, A., M. Das, and S. Satyanarayana, Preparation and characterization of amyloglucosidase adsorbed on activated charcoal. Journal of Molecular Catalysis B: Enzymatic, 2000. 10(5): p. 471-476.

[16]Mansfeld, J. and A. Schellenberger, Invertase immobilized on macroporous polystyrene: properties and kinetic characterization. Biotechnology and Bioengineering, 1987. 29(1): p. 72-78.

[17]Pereira, E., G. Zanin, and H. Castro, Immobilization and catalytic properties of lipase on chitosan for hydrolysis and esterification reactions. Brazilian Journal of Chemical Engineering, 2003. 20(4): p. 343-355.

[18]Li, G.-Y., et al., Production of (R)-mandelic acid by immobilized cells of Saccharomyces cerevisiae on chitosan carrier. Process Biochemistry, 2007. 42(10): p. 1465-1469.

[19]Su, E., et al., Immobilization of β-glucosidase and its aroma-increasing effect on tea beverage. Food and Bioproducts Processing, 2010. 88(2-3): p. 83-89.

[20]Ahmad, R. and M. Sardar, Enzyme immobilization: an overview on nanoparticles as immobilization matrix. Biochemistry and Analytical Biochemistry, 2015. 4(2): p. 1.

[21]Ansari, S.A. and Q. Husain, Potential applications of enzymes immobilized on/in nano materials: A review. Biotechnology Advances, 2012. 30(3): p. 512-523.

[22]Gupta, M.N., et al., Nanomaterials as matrices for enzyme immobilization. Artificial Cells, Blood Substitutes, and Biotechnology, 2011. 39(2): p. 98-109.

[23]Bai, Y.-X., et al., Covalent immobilization of triacylglycerol lipase onto functionalized nanoscale SiO2 spheres. Process Biochemistry, 2006. 41(4): p. 770-777.

[24]Zhang, S., et al., Immobilization of glucose oxidase on gold nanoparticles modified Au electrode for the construction of biosensor. Sensors and Actuators B: Chemical,

2005. 109(2): p. 367-374.

[25]Lv, Z., et al., Immobilization and performance of penicillin G acylase on magnetic $Ni_{0.7}Co_{0.3}Fe_2O_4$@SiO_2-CHO nanocomposites. Journal of Microbiology and Biotechnology, 2019.

[26]Wu, W., Q. He, and C. Jiang, Magnetic iron oxide nanoparticles: synthesis and surface functionalization strategies. Nanoscale Research Letters, 2008. 3(11): p. 397.

[27]Song, J., et al., Attachment of enzymes to hydrophilic magnetic nanoparticles through DNA-directed immobilization with enhanced stability and catalytic activity. New Journal of Chemistry, 2018. 42(11): p. 8458-8468.

[28]Cabrera, M.P., et al., Polyaniline-coated magnetic diatomite nanoparticles as a matrix for immobilizing enzymes. Applied Surface Science, 2018. 457: p. 21-29.

[29]Joo, H. and J.-h. Lee, Polyaniline nanofiber coated monolith reactor for enzymatic bioconversion. Journal of Molecular Catalysis B: Enzymatic, 2010. 67(3-4): p. 179-183.

[30]Huang, J. and R.B. Kaner, Nanofiber formation in the chemical polymerization of aniline: a mechanistic study. Angewandte Chemie International Edition, 2004. 43(43): p. 5817-5821.

[31]Bhadra, S., et al., Progress in preparation, processing and applications of polyaniline. Progress in Polymer Science, 2009. 34(8): p. 783-810.

[32]Boeva, Z.A. and V.G. Sergeyev, Polyaniline: synthesis, properties, and application. Polymer Science Series C, 2014. 56(1): p. 144-153.

[33]Zhang, Z., M. Wan, and Y. Wei, Electromagnetic functionalized polyaniline nanostructures. Nanotechnology, 2005. 16(12): p. 2827.

[34]Rahim, M.A., et al., Coordination-driven multistep assembly of metal–polyphenol films and capsules. Chemistry of Materials, 2014. 26(4): p. 1645-1653.

[35]Ejima, H., et al., One-step assembly of coordination complexes for versatile film and particle engineering. Science, 2013. 341(6142): p. 154-157.

[36]Guo, H., et al., A one-step rapid assembly of thin film coating using green coordination complexes for enhanced removal of trace organic contaminants by membranes. Environmental Science & Technology, 2017. 51(21): p. 12638-12643.

[37]Batul, R., et al., Recent progress in the biomedical applications of polydopamine nanostructures. Biomaterials Science, 2017. 5(7): p. 1204-1229.

[38]Seok, S., et al., Dopamine-induced Pt and N-doped carbon@silica hybrids as high-performance anode catalysts for polymer electrolyte membrane fuel cells. RSC Advances, 2014. 4(80): p. 42582-42584.

[39]Cui, J., et al., Shielding effects of Fe^{3+}-tannic acid nanocoatings for immobilized enzyme on magnetic Fe_3O_4@silica core shell nanosphere. Chemical Engineering Journal, 2018. 343: p. 629-637.

[40]Jiang, X., Y. Wang, and M. Li, Selecting water-alcohol mixed solvent for synthesis of polydopamine nano-spheres using solubility parameter. Scientific Reports, 2014. 4: p. 6070.

[41]Kim, R.E., et al., Enzyme adsorption, precipitation and crosslinking of glucose oxidase and laccase on polyaniline nanofibers for highly stable enzymatic biofuel cells. Enzyme and Microbial Technology, 2014. 66: p. 35-41.

[42]Kim, H., et al., Immobilization of glucose oxidase into polyaniline nanofiber matrix for biofuel cell applications. Biosensors and Bioelectronics, 2011. 26(9): p. 3908-3913.

[43]Zhong, Q. and C.E. Glatz, Enzymatic assay method for evaluating the lipase activity in complex extracts from transgenic corn seed. Journal of Agricultural and Food Cemistry, 2006. 54(9): p. 3181-3185.

[44]Pliego, J., et al., Monitoring lipase/esterase activity by stopped flow in a sequential injection analysis system using p-nitrophenyl butyrate. Sensors, 2015. 15(2): p. 2798-2811.

[45]Zhang, X., S. Stefanick, and F.J. Villani, Application of microreactor technology in process development. Organic Process Research & Development, 2004. 8(3): p.

455-460.

[46]Veeramani, M., S. Narasimhan, and N. Bhatt, Identification of reaction systems using spectroscopic measurements and micro-reactors, in Computer Aided Chemical Engineering. 2018, Elsevier. p. 931-936.

[47]Eed, J., Factors affecting enzyme activity. Essai, 2012. 10(1): p. 19.

[48]Robinson, P.K., Enzymes: principles and biotechnological applications. Essays in Biochemistry, 2015. 59: p. 1-41.

[49]Ferreira, C.M., et al., (Un) suitability of the use of pH buffers in biological, biochemical and environmental studies and their interaction with metal ions–a review. RSC Advances, 2015. 5(39): p. 30989-31003.

[50]Aydar, A.Y., Utilization of response surface methodology in optimization of extraction of plant materials. Statistical Approaches With Emphasis on Design of Experiments Applied to Chemical Processes. InTech, 2018: p. 157-169.

[51]Boyacı, İ.H., A new approach for determination of enzyme kinetic constants using response surface methodology. Biochemical Engineering Journal, 2005. 25(1): p. 55-62.

[52]Lee, C.H., et al., A new analytical method to determine non-steroidal anti-inflammatory drugs in surface water using in situ derivatization combined with ultrasound-assisted emulsification microextraction followed by gas chromatography–mass spectrometry. Talanta, 2014. 129: p. 552-559.

[53]Grodowska, K. and A. Parczewski, Analytical methods for residual solvents determination in pharmaceutical products. Acta Pol. Pharm, 2010. 67(1): p. 13-26.

[54]Glogauer, A., et al., Identification and characterization of a new true lipase isolated through metagenomic approach. Microbial Cell Factories, 2011. 10(1): p. 54.

[55]Guan, H., et al., Polyaniline nanofibers obtained by interfacial polymerization for high-rate supercapacitors. Electrochimica Acta, 2010. 56(2): p. 964-968.

[56]Du, Y., K. Cai, and S.Z. Shen, Facile preparation and characterization of graphene nanosheet/polyaniline nanofiber thermoelectric composites. Functional Materials

Letters, 2013. 6(05): p. 1340002.

[57]Kumar, A., et al., Synthesis and characterization of hybrid PANI/MWCNT nanocomposites for EMI applications. Polymer Composites, 2018. 39(11): p. 3858-3868.

[58]Rafeeq, S.N. and W.Z. Khalaf, Preparation, characterization and electrical conductivity of doped polyaniline with (HCL and P-TSA). Engineering and Technology Journal, 2015. 33(7 Part (B) Scientific): p. 1220-1231.

[59]Bachhav, S. and D. Patil, Synthesis and characterization of polyaniline-multiwalled carbon nanotube nanocomposites and its electrical percolation behavior. Am J Mater Sci, 2015. 5(4): p. 90-95.

[60]Sim, B., H. Chae, and H. Choi, Fabrication of polyaniline coated iron oxide hybrid particles and their dual stimuli-response under electric and magnetic fields. Express Polymer Letters, 2015. 9(8).

[61]Dhachanamoorthi, N., et al., Facile preparation and characterization of polyaniline-iron oxide ternary polymer nanocomposites by using "mechanical mixing" approach. Mechanics, Materials Science & Engineering MMSE Journal. Open Access, 2017. 9.

[62]Çakar, S. and M. Özacar, Fe–tannic acid complex dye as photo sensitizer for different morphological ZnO based DSSCs. Spectrochimica Acta Part A: Molecular and Biomolecular Spectroscopy, 2016. 163: p. 79-88.

[63]Li, Y., et al., Iron-tannic acid nanocomplexes: facile synthesis and application for removal of methylene blue from aqueous solution. Digest Journal of Nanomaterials & Biostructures (DJNB), 2016. 11(4).

[64]Alonso, P.E.d.G., Alternative synthesis methods of electrically conductive bacterial cellulose-polyaniline composites for potential drug delivery application. 2017.

[65]Luo, H., et al., Facile synthesis of novel size-controlled antibacterial hybrid spheres using silver nanoparticles loaded with poly-dopamine spheres. RSC Advances, 2015. 5(18): p. 13470-13477.

[66]Batul, R., et al., Synthesis of polydopamine nanoparticles for drug delivery applications. Microscopy and Microanalysis, 2018. 24(S1): p. 1758-1759.

[67]Rios, N.S., et al., Increasing the enzyme loading capacity of porous supports by a layer-by-layer immobilization strategy using PEI as glue. Catalysts, 2019. 9(7): p. 576.

[68]Altun, S., et al., A facile and effective immobilization of glucose oxidase on tannic acid modified $CoFe_2O_4$ magnetic nanoparticles. Colloids and Surfaces B: Biointerfaces, 2015. 136: p. 963-970.

[69]Perna, R.F., et al., Effects of triton X-100 and PEG on the catalytic properties and thermal stability of lipase from Candida Rugosa free and immobilized on glyoxyl-agarose. The Open Biochemistry Journal, 2017. 11: p. 66.

초록

니켈 foam을 이용한 우수한 고정화 재료 합성 및 고정화효소 특성 분석

사 방지

지도 교수: 이중헌 교수

화학공학과

조선대학교 대학원

생명 공학, 재료, 화학 및 다른 표면개질 방법의 지속적인 개발로 인해 새로운 재료들이 계속 등장하고 있어 고정화 기술 연구를 위한 담체 원료들이 많이 개발되고 있다. 니켈 폼 (Ni-foam)은 가격이 저렴하고 다루기 쉬우며 스펀지와 같은 다공성 구조로 인해 베이스 담체 재료로 매우 적합하다. 따라서 본 연구에서는 Ni-foam을 담체 재료로 사용하였고 polyaniline nanofibers (PANI), polyaniline magnetic particles (PAMP), tannin iron ion complex (TA@$FeCl_3$_$6H_2O$), polydopamine (PDA)을 포함한 다양한 폴리머 재료로 Ni-foam 표면을 코팅하였다. 이들은 작용기를 가지고 있어 화학적 가교법으로 효소를 고정화하기가 더 쉽다. PANI, PAMP, TA@$FeCl_3$_$6H_2O$, 및 PDA 합성 단계에서 Ni-foam을 넣어 Ni-foam 표면을 코팅하였다. 이전에, 이러한 폴리머 물질들은 효소 고정화 재료로서 분산 된 입자 형태로 사용된다. 이러한 방법은 회수가 어렵다는 단점이 있다. 그러나 Ni-foam을 사용할 경우 반응 용액으로부터 쉽게 회수가 가능하고, 반응을 쉽게 제어할 수 있다는 장점이 있다. 고정화 된 효소 및 담체 특성은 fourier transform infrared (FTIR-ATR) spectrophotometer, scanning electron microscope (SEM), 및 UV/Visible spectrophotometer를 사용하여 특성화되었다.

목적으로 하는 폴리머들이 Ni-foam 표면에 합성이 되었는지 FTIR-ATR 분석법을 통해 확인하였고, SEM 이미지를 통해 표면이 개질된 Ni-foam에 효소가 고정화되었음을 확인할 수 있었다.

고정화 된 lipase (LIP) 및 glucose oxidase (GOx)의 안정성을 분석 하였다. 그 결과 순수한 Ni-foam에 고정화된 GOx의 활성은 한 달 후에 거의 사라졌다. 그러나 PANI, PAMP, TA@$FeCl_3$_$6H_2O$ 및 PDA로 코팅된 Ni-foam에 GOx를 고정화 하였을 때 잔류 활성은 각각 50.9%, 70.4%, 72.1%, 73.4%였다. 순수한 Ni-foam에 고정화 된 LIP의 초기 활성은 PAMP, PANI, PDA로 코팅된 것보다 높았지만 안정성은 좋지 않았다. TA@$FeCl_3$_$6H_2O$상의 고정화 된 LIP는 가장 안정적이고 우수한 잔류 효소 활성을 가졌으며, 이어서 PDA, PAMP였다. 1 개월 후, 순수한 Ni-foam 과 PANI, PAMP, TA@$FeCl_3$_$6H_2O$ 및 PDA로 코팅된 Ni-foam에 고정화된 효소의 잔류 활성은 각각 83.1%, 73.3%, 93.4%, 90.1% 및 98.3%였다.

600 μL 용량의 PFR 마이크로 반응기가 개발되었고, 관형 반응기 안에 Ni-foam에 고정화된 효소가 사용되었다. 실험 결과, PDA-GOx 및 PAMP-GOx는 양호한 작동 안정성을 보였다. PDA-GOx를 사용한 포도당 전환율은 172 시간 후에 84.6±4.7%에서 18.4±2.3%로 감소한 반면, PAMP-GOx는 82.1±1%에서 22.2±4.4%로 감소했다. LIP의 경우, 기질 4-NPB의 가수 분해 생성물이 pH에 의해 크게 영향을 받아 pH를 6.5로 고정하고 마이크로 PFR을 사용하여 실온에서의 작동 안정성을 보았다. 그 결과 24 일 연속 작동 후에도 전환율이 변하지 않았다.

요약하면, Ni-foam의 표면 개질은 효소 반응 공정의 안정성을 증가시킬 뿐만 아니라 공정을 경제적으로 가능하게 하였다.

주제어 : 폴리아닐린 나노 섬유 (PANI), 폴리아닐린 자성 입자 (PAMP), 탄닌 철 이온 복합체 (TA@$FeCl_3$_$6H_2O$), 폴리 도파민 (PDA), 니켈 폼 (Ni-foam), 리파제 (LIP), 포도당 산화 효소 (GOx)